Field Guides

Historical surface faulting and paleoseismology of the central Nevada seismic belt

S. John Caskey, John W. Bell and D. Burton Slemmons

Field Guides 2000;2;23-44
doi: 10.1130/0-8137-0002-7.23

Geological Society of America
Field Guide 2
2000

Historical surface faulting and paleoseismology of the central Nevada seismic belt

S. John Caskey
Department of Geosciences, San Francisco State University, San Francisco, California, USA
John W. Bell
Nevada Bureau of Mines and Geology, Mackay School of Mines, USA
University of Nevada, Reno, Nevada
D. Burton Slemmons
2905 Autumn Haze Lane, Las Vegas, Nevada, USA

INTRODUCTION

This three-day field trip will examine the nature of contemporary tectonic processes in the western Basin and Range province by focusing on the historical faulting and paleoseismology of the central Nevada seismic belt (CNSB) (Fig. 1). The trip begins in Reno and includes travel through Fallon, Nevada to major faulting sites in the 1954 Rainbow Mountain, Fairview Peak, and Dixie Valley rupture area ~125 km east of Reno (Fig. 2). The principal topics addressed by this trip will include:

The structural pattern, distribution, and characteristics of surface faulting and secondary effects associated with large-magnitude historical earthquakes as they bear on the nature of modern tectonic processes in the CNSB.

The paleoseismicity of the historical fault zones within the CNSB, the long-term slip rate, and recurrence characteristics determined from exploratory trenching, and their relevance to other contemporary crustal strain measurements, such as GPS.

The variations and similarities of fault slip rates both within and outside of the CNSB and the implications for seismic hazard characterization of the western Basin and Range, including the evidence that low slip rate faults may be sources of high seismic hazard.

The CNSB (Fig.1) was named by Wallace (1984) based on the belt-like clustering of multiple, large-magnitude, historical surface-rupturing earthquakes. These events comprise a north-trending zone of semicontinuous, overlapping surface ruptures that extend northward through eastern California and central Nevada. The CNSB comprises seven major surface-rupturing events including: the 1872 Owens Valley (M_s7.7); 1915 Pleasant Valley (M_s7.7); 1932 Cedar Mountain (M_s7.2); 1954 Rainbow Mountain-Stillwater sequence (M_s 6.3, M_s 7.0); 1954 Fairview Peak (M_s7.2); and 1954 Dixie Valley (M_s 6.8) earthquakes. Three smaller events include the 1903 Wonder (M 6.0?), 1934 Excelsior Mountain (M_s 6.3), and 1954 Four Mile Flat (M 6.0?) events. These events collectively constitute a major portion of the contemporary tectonic activity in the Basin and Range province. Recent GPS studies by Thatcher et al. (1999) show that levels of modern crustal deformation across the CNSB continue to be elevated with respect to adjacent regions.

DAY 1. RENO TO RAINBOW MOUNTAIN AND FAIRVIEW PEAK

Directions: Depart Reno on I–80 traveling east through Truckee Meadows and the Truckee River Canyon. Mileage begins at the I–80/US 395 interchange.

The recent geologic history of the route between Reno and Fallon is dominated by an extensive mid to late Quaternary glacial and pluvial sequence that forms the stratigraphic framework for interpreting the structure and tectonics of the region. Reno is situated within an alluvium-filled, down-faulted structural basin between the Carson Range block of the Sierra Nevada on the west and the Virginia Range on the east. The basin, locally referred to as the Truckee Meadows, contains >300 m of Plio–Pleistocene age sediment. The Truckee River, an antecedent stream originating in mid to late Tertiary time, flows from Lake Tahoe through Reno to Pyramid Lake, and it has been the source of much of the alluvial fill within the basin. During the Quaternary, extensive glacial outwash of Donner Lake, Tahoe, and Tioga age derived from glaciers in the Lake Tahoe basin, was deposited in the Truckee Meadows. No numerical age data have been obtained from Donner Lake and Tahoe age deposits in the northern Sierra Nevada region, but they are generally taken to be of isotope stage 6 age and older (>130 ka). Deposits of Tioga and younger age have been ^{14}C dated in the eastern part of the Truckee Meadows at between 7–26 ka (Bell and Bonham, 1987). Lacustrine deposits of the Lake Lahontan pluvial sequence that occur farther to the east (Morrison, 1964) did not extend into the Truckee Meadows.

Caskey, S.J., Bell, J.W., and Slemmons, D.B., Historical surface faulting and paleoseismology of the central Nevada seismic belt, *in* Lageson, D.R., Peters, S.G., and Lahren, M.M., eds., Great Basin and Sierra Nevada: Boulder, Colorado, Geological Society of America Field Guide 2, p. 23–44.

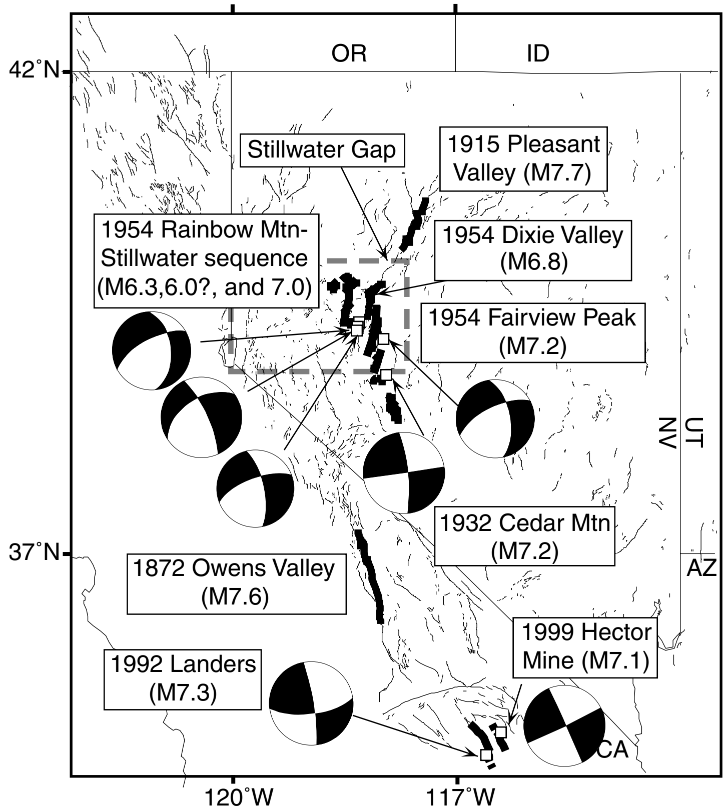

Figure 1. Map showing surface ruptures (bold lines) and focal mechanisms reported for major historical earthquakes of the central Nevada–eastern California seismic belt. Other Quaternary faults of the Basin and Range are shown as thinner lines. Compressional quadrants of focal mechanism are black. Focal mechanisms are from Doser (1986) and the National Earthquake Information Center. Area of Figure 2 is shown by the gray box. Within the central Nevada seismic belt, right-normal-oblique surface ruptures of 1954 Rainbow Mountain–Fairview Peak sequence mark a transition between dominantly right-lateral events to the south within the northwest-trending Walker Lane belt (Stewart, 1988), and the dominantly dip-slip Dixie Valley and Pleasant Valley earthquakes to the north, where the Basin and Range is characterized by a consistent north- to northeast-trending structural grain.

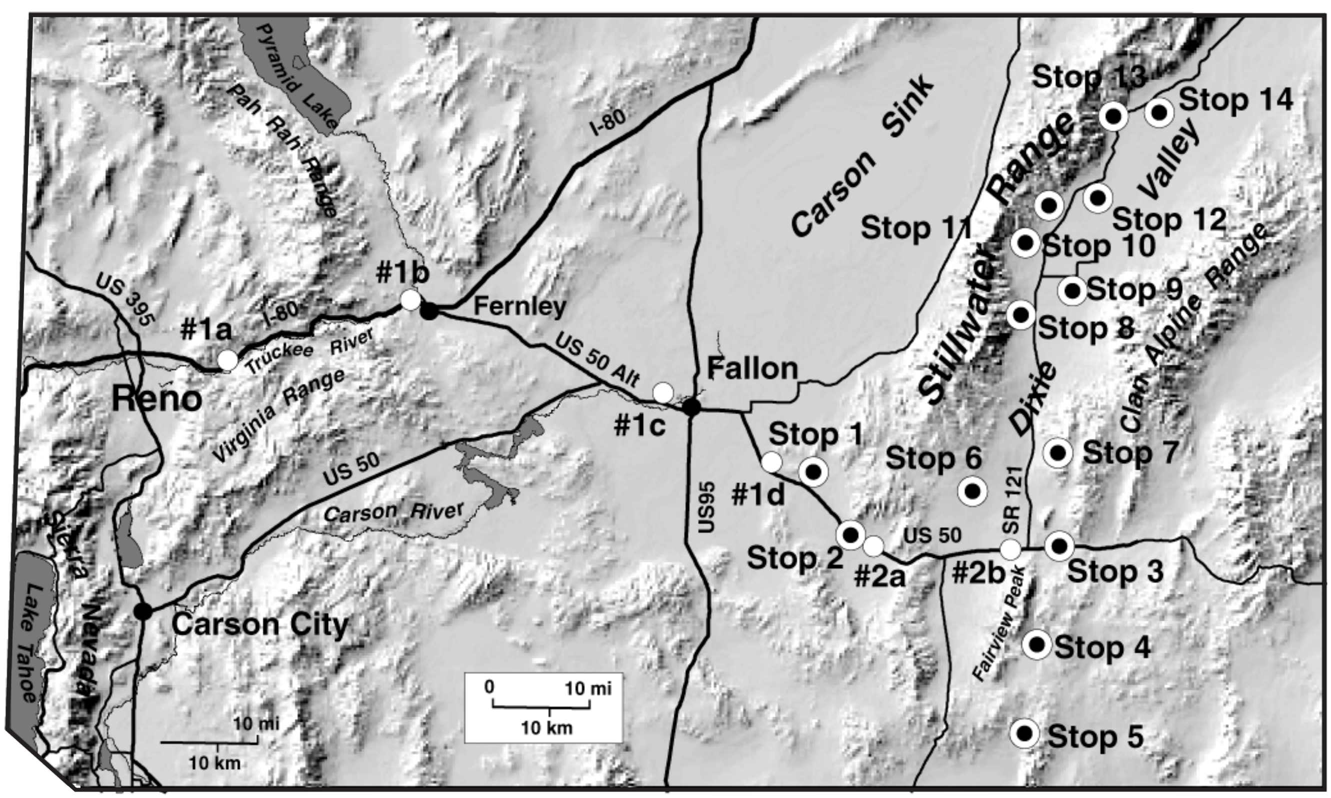

Figure 2. Location map of the field trip region showing locations of field trip stops. Drive-by stops marked as #1a-d, #2a-b.

Drive-by stop #1a: Pluvial Lake Lahontan features

Directions: Proceed 8.8 mi (14.2 km) east from I–80.US 395 interchange to Mustang following the Truckee River Canyon.

The fluvial terraces between the highway and the river to the south at Mustang are composed of glacial outwash interbedded with lacustrine deposits associated with the westernmost extent of pluvial Lake Lahontan upstream along the Truckee Canyon. The first low terrace just off the interstate to the south is composed of Donner Lake outwash, and the next lower terrace toward the river is Tahoe outwash. Prior to extensive grading, the Tahoe outwash gravels were observed interbedded with silt and clay deposits of the Eetza Formation, a pluvial sequence of isotope stage 6 age (Morrison and Davis, 1984; Morrison, 1991).

For the next 30 km the Truckee Canyon is incised in the Lahontan sedimentary sequence, and outcrops of the light-colored well-bedded silt and clay units of the Eetza Formation and the younger Sehoo Formation (late glacial, stage 2 age) are seen in the roadcuts.

Drive-by stop #1b: Pyramid Lake–Olinghouse fault zones

Directions: Proceed from Mustang east for 20.7 mi (33.3 km) to the east exit of the Truckee Canyon near Wadsworth, Nevada.

At this location, the Truckee River turns north and flows into Pyramid Lake and becomes more deeply incised into a thick sequence of Lake Lahontan deposits. The Truckee River drainage between Wadsworth and Pyramid is structurally controlled by the Pyramid Lake fault zone, one of the northern segments of the right-lateral Walker Lane, a 700-km-long zone of late Cenozoic strike-slip structure in the western Basin and Range. The Pyramid Lake fault zone cuts the high shoreline and beach deposits of late Sehoo age (~13 ka) and exhibits widespread geomorphic evidence of strike-slip tectonics, including offset stream channels, rhomb-shaped depressions, sag ponds, and pressure ridges. Exploratory trenching of the zone by Anderson and Hawkins (1984) indicated that at least 4 faulting events offset Mazama ash deposits (6.85 ka), with a slip rate of >1 mm/yr.

The Olinghouse fault zone is located ~5 km to the northwest. The fault is east-northeast–striking and conjugate to the Pyramid Lake fault zone. Between Wadsworth and Reno, the Olinghouse fault lies a few kilometers north of I–80 and exhibits surficial evidence of left-lateral strike-slip motion in late Quaternary alluvial deposits, and it is believed to be the location of a surface-rupturing earthquake (M 6.7) in 1869 (Sanders and Slemmons, 1979).

Drive-by Stop #1c: Late Quaternary chronostratigraphy of the Fallon area

Directions: Proceed from Wadsworth east for 4 mi (6.4 km) to the East Fernley exit and follow U.S. 50 east for 30 km to Fallon.

Fallon is located in the southern Carson Desert, the type locale for the extensive stratigraphic studies of Lake Lahontan by Morrison (1964), which forms the basis for much of the chronostratigraphy in western Nevada. Lake Lahontan occupied >21,000 km^2 in the western Basin and Range, first during the mid-Pleistocene and then later during the late glacial period, principally between 13–30 ka. The pluvial sequence includes alternating intervals of deep-water lacustrine deposition with subaerial alluvial deposition beginning ~1 Ma. The reader is referred to the most recent, detailed description of Lake Lahontan stratigraphy contained in Morrison (1991).

The principal Lake Lahontan stratigraphic units in the Fallon region include the lacustrine Eetza Formation (130–300 ka), the subaerial Wyemaha Formation (30–130 ka), and the Sehoo Formation (13–30 ka). The Sehoo lake interval was followed by subaerial deposition of the Turupah Formation in the mid Holocene, and the occupation of a small lake phase in late Holocene time, marked by the Fallon Formation.

Fallon lies within a large structural basin, the Carson Sink, that is likely a pull-apart feature of the dextral-slip Walker Lane zone that lies on the western margin of the sink. The basin contains hundreds of meters of lacustrine sediment, and during the 1954 Rainbow Mountain earthquakes, buildings and fields in Fallon were widely damaged largely due to amplified ground motion and liquefaction.

Overview of the 1954 Rainbow Mountain–Stillwater earthquake sequence

The Rainbow Mountain area experienced three strong earthquakes in 1954; two on July 6 and one on August 24 (Figs. 1 and 3). The initial M_s6.3 July 6 event (the Rainbow Mountain earthquake) produced a generally linear, 20-km-long zone of discontinuous, north-northeast–trending ruptures along the east-dipping Rainbow Mountain fault (Tocher, 1956). The fault bounds the eastern escarpment of Rainbow Mountain, a moderately west-tilted fault block comprised of late Tertiary volcanic and sedimentary rocks (Stewart and Carlson, 1978). A second (M_w6.0) July 6 event (herein referred to as the Four Mile Flat earthquake) followed the initial event by ~11 hours (Doser, 1986). Doser's 1986 relocation for this event (Fig. 3) together with anecdotal information (Tocher, 1956) (discussed below) indicates that this event is likely associated with small ruptures along the northern margin of Four Mile Flat (Tocher, 1956) and previously unmapped minor ruptures along the Four Mile Flat fault (Caskey et al., in review). The third event in the sequence, the M_s7.0 Stillwater earthquake, occurred on August 24, and produced a 52-km-long zone of discontinuous ruptures mostly within Carson Sink, north of, and along-strike with the initial 6 July ruptures (Tocher, 1956). The earthquake also produced several small (0.5–1.5 km long) breaks that overlap with and locally reactivated the initial July 6 ruptures (Tocher, 1956).

Using recent large-scale low-sun-angle aerial photography and 1957 vintage aerial photos, Caskey et al. (in review) recently extended the known rupture length of the earthquake sequence from 40–70 km. For the most part, the 1954 scarps are still well preserved in the arid desert environment. However, scarps in the central and northern parts of Carson Sink are no

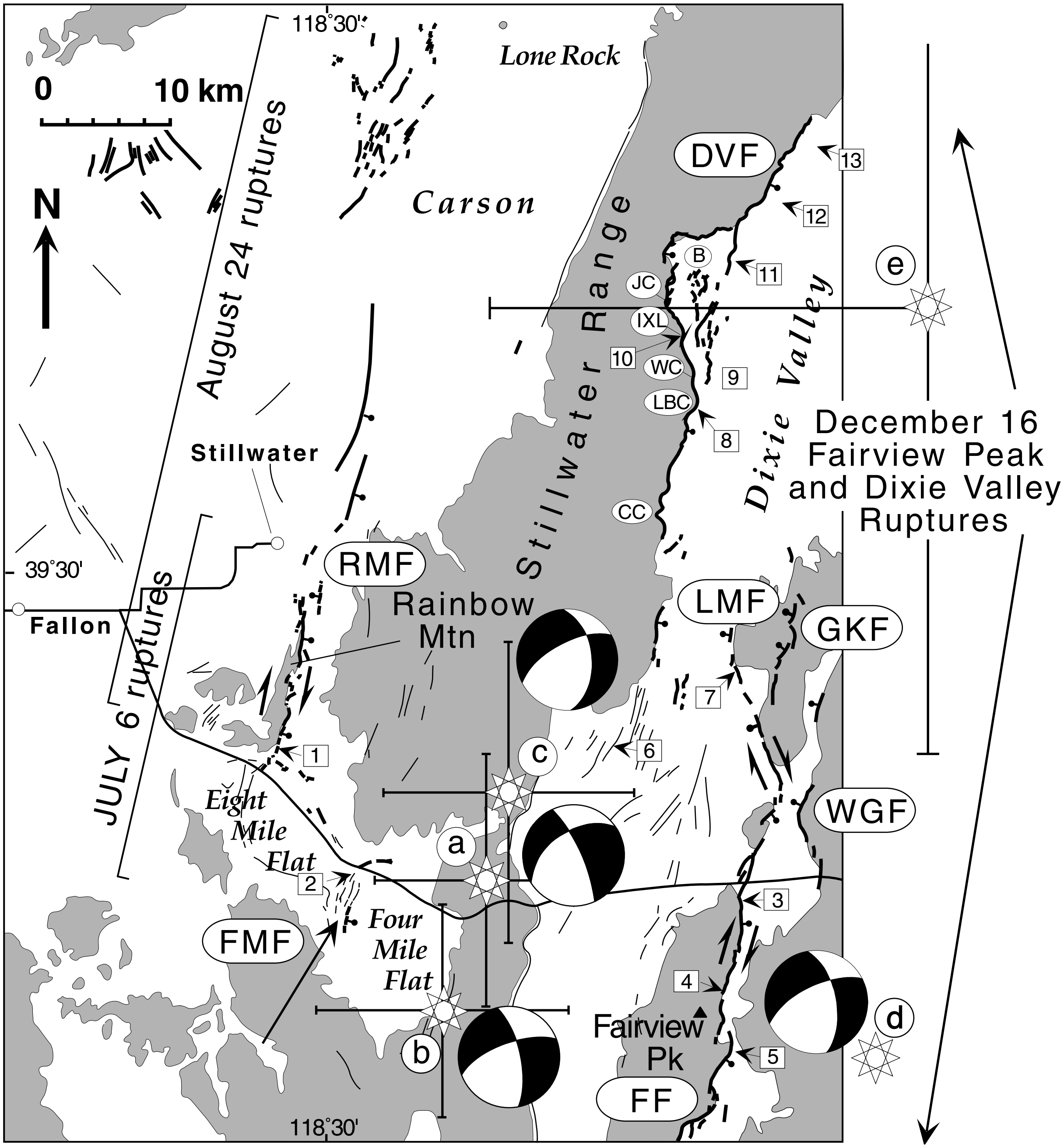

Figure 3. Rupture zones of the 1954 earthquake sequence (bold lines) (after Bell, 1984; Caskey et al., 1996; Tocher, 1956). Base map shows Quaternary faults (thinner lines), bedrock (shaded), and alluvium (white) (modified from Stewart and Carlson (1978) and Bell (1984). Epicenters (stars) and focal mechanisms for the 1954 sequence are taken from Doser (1986). Compressional quadrants for focal mechanisms are black. Letters correspond to locations of events in the order of occurrence: a) the initial (M_s6.4) July 6 (Rainbow Mountain), b) a second (M_w6.0) July 6 (Four Mile Flat) c) the (M_s7.0) August 24 (Stillwater) event, d) the (M_s7.2) December 16 (Fairview Peak), and e) the (M_s6.8) December 16 (Dixie Valley) earthquakes. Field trip Stops 1–13 are shown numbered in boxes. Abbreviations for faults; DVF—Dixie Valley, GKF—Gold King, FF—Fairview, FMF—Four Mile Flat, LMF—Louderback Mountains, and RMF—Rainbow Mountain faults. Abbreviations for locations referred to text; B—The Bend, CC—Coyote Canyon, IXL—IXL Canyon, JC—James Canyon, LBC—Little Box Canyon, WC—Willow Canyon.

longer preserved due to the incohesive nature of surficial deposits in the area, and because portions of the basin are either under water or have intermittently been inundated since the earthquakes.

Maximum vertical offsets across surface ruptures ranged from 35–76 cm (Tocher, 1956). Caskey et al. (in review) reported previously unrecognized right-lateral stream channel offsets of up to 100 cm locally along the Rainbow Mountain fault. Other field evidence for a lateral slip component includes pronounced left-stepping en echelon scarps (i.e., Riedel shears) and a well-preserved 100-m-long mole track on the playa surface in Carson Sink. The lateral offsets were observed along a section of the fault that initially broke during the July 6 event (Tocher, 1956). However, assigning the lateral offsets to a specific event is problematic because the August 24 event reactivated portions of the fault as far south as the lateral slip measurements. Nevertheless, the strong right-slip component is consistent with focal plane solutions for the events (Doser, 1986) (Fig. 3) and recent geodetic models (Hodgkinson et al., 1996). The newly recognized lateral offsets and extended length of rupture brings geological estimates of seismic moment release (Caskey, et al., in review) into closer accord with previously reported seismological estimates (Doser, 1986).

Finally, there is a mismatch between the north-northeast–striking surface ruptures, and the north-northwest fault strikes delineated by focal mechanisms. This relationship is also true for the1954 Fairview Peak and aspects of the1932 Cedar Mountain earthquakes (Bell et al., 1999). It is possible that fault surfaces in the region, particularly those within the transition between the northwest-trending Walker Lane belt to the west and the northeast-trending structural grain of the central Great Basin, may rotate and fan upward from focal depths in the fashion of Riedel shears above lateral slip faults (e.g., Naylor et al., 1986).

Drive by Stop #1d: Grimes Point archeological area

Directions: From U.S. Highway 95 intersection, continue east from Fallon along U.S. Highway 50 for 10 mi (16 km)

Grimes Point archeological area is one of the largest and most accessible petroglyph sites in northern Nevada, hosting >150 basalt boulders with >1000 pieces of rock art. Most of the petroglyphs date between 5000 B.C. and 1500 A.D. and are attributed to the native American people of the Northern Paiutes (Cattail-eaters or "Toidikadi") who used abundant marsh resources to supply most of their material needs. The area also marks the burial site of Spirit Cave Man, the oldest known mummified ancient American, dated at 9400 ybp. Spirit Cave Man along with Kennewick Man (9200 ybp) found along the banks of the Columbia River in Washington, may provide clues to the earliest immigrants of the Western Hemisphere.

Stop 1. Wave-modified Paleoscarp (?) and 6 July 1954 fault ruptures

Directions: From Grimes Point archeological area, continue east along U.S. Highway 50 for 4.6 mi (7.4 km); turn north on dirt road ~0.4 mi (0.6 km) southeast of Salt Wells Brothel (on south side of road); follow road 2.5 mi (4 km) and park on shoulder; hike ~100 m west up to small 1 m escarpment.

The entire Rainbow Mountain fault trace lies at an elevation below high level shorelines of pluvial Lake Lahontan, which reached a maximum elevation of ~1332 m (~4370 ft) ~13,000 ybp (Morrison, 1964; Benson et al., 1992; Adams and Wesnousky, 1998). Hence, geomorphic evidence for pre-Holocene paleoseismicity along the Rainbow Mountain fault has largely been obscured by paleoshoreline processes. However, at this location what appears to be a wave-modified paleoscarp is still preserved (Fig. 4). This section of the fault initially broke during the 6 July 1954 Rainbow Mountain event. Small 1954 scarps with vertical separations of 20–25 cm can be traced along the entire base of the paleoscarp (?). Net vertical separation across the apparent compound scarp is ~1 m. The age of the penultimate event is presumed to be pre-13 ka.

Stop 2. Channel exposure and Holocene paleoseismicity on the Four Mile Flat fault

Directions: Return to U.S. Highway 50; continue southeast for 7.3 mi (11.8 km); turn south on dirt road that heads out to the

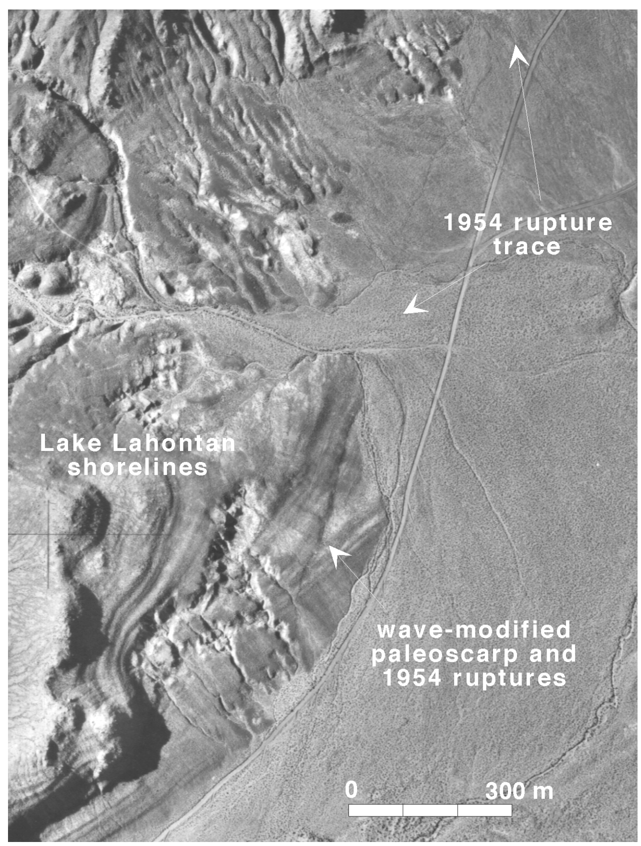

Figure 4. Low-sun-angle photograph of wave modified paleoscarp(?), 1954 fault ruptures and latest Pleistocene to early Holocene Lake Lahontan shorelines along southern part of the Rainbow Mountain fault (Stop 1). Small 20–25 cm high scarps formed along the base of the paleoscarp during the initial July 6, 1954 (Rainbow Mountain) earthquake.

Huck salt mine; park and hike south across salt flat ~0.3 km to exposure at sharp bend along inset channel.

The Four Mile Flat fault (FMFF) separates Eight Mile Flat to the northwest from the down-dropped Four Mile Flat to the southeast (Fig. 3). The fault consists of several north-trending, subparallel, and overlapping scarps on the playa surface that extend and curve eastward along the northern margin of Four Mile Flat for a total length of 6–8 kms (Caskey et al., in review).

Tocher (1956) reported that "many people" observed a large cloud of dust arising from this area at the time of the second 6 July 1954 (Four Mile Flat) earthquake. In addition, numerous cracks and graben were first noticed across U.S. Highway 50 along the FMFF trace following the second July 6 event (Tocher, 1956). Caskey et al. (in review) reported small (15 cm high) historical scarps along a several-kilometer–long section of the FMFF ~3 km south of this location (Fig. 3). These historic ruptures as well as the prehistoric trace of the FMFF remained unrecognized until the Caskey et al. field investigation of the earthquake sequence. The anecdotal evidence, together with the new mapping and Doser's (1986) relocation of the second July 6 event (Fig. 3), indicate that this earthquake probably occurred on the FMFF. Models of static stress changes associated with the initial July 6 (Rainbow Mountain) earthquake (Caskey, unpublished) suggest that failure stress was enhanced on the Four Mile Flat fault, and that these stress changes probably contributed to the subsequent triggering of the Four Mile Flat earthquake.

The FMFF apparently did not rupture at the surface at this location in 1954. Here, the fault is expressed as a very subdued paleoscarp that exhibits 0.6 m of vertical offset of the playa surface (Fig. 5). Farther south, the playa surface is down-dropped to the east along a more eastern strand of the fault zone by as much as 2 m of prehistoric vertical displacements.

The channel cut at this location exposes a complex, ~15 m wide fault zone that disrupts lacustrine strata comprised of 1.5 m of greenish clay and three latest Pleistocene to possibly mid-Holocene tephra layers (Sarna-Wojcicki, personal commun.) deposited during the late Sehoo and possibly Holocene lake intervals (Fig. 5). The tephra layers provide distinct stratigraphic markers that record evidence for both the timing and vertical offsets associated with two paleoseismic events, only the most recent of which appears to be associated with the playa paleoscarp (Fig. 5).

We interpret a sequence of events for the FMFF as follows: 1) deposition of lacustrine clays and the three tephra layers during the latest Pleistocene to mid-Holocene(?); 2) A subsequent surface rupturing earthquake along the FMFF that vertically displaced the three lower tephra layers by ~1.0 m; 3) erosional leveling of the playa surface (enough to remove an approximately 1.0-m-high scarp and uplifted strata containing the upper two tephra (i.e., the tephra couplet; 4) a second faulting event responsible for forming the 0.6-m-high playa scarp; and 5) localized reactivation of the FMFF in areas both to the north and south of this location during the 1954 earthquake sequence (see Fig. 5 caption for a discussion of stratigraphic and structural details). Preservation of a 0.6-m-high scarp on the playa surface indicates that the most recent paleoseismic event probably occurred in the mid to late Holocene.

Drive by Stop #2a Sand Mountain

Directions: Return to U.S. Highway 50; continue southeast for ~1.0 mi (1.6 km).

The large sand dune at 10:30 is Sand Mountain, which is ~180 m in height. The quartz sands have an original Sierran provenance (Nick Lancaster, Desert Research Institute, personal

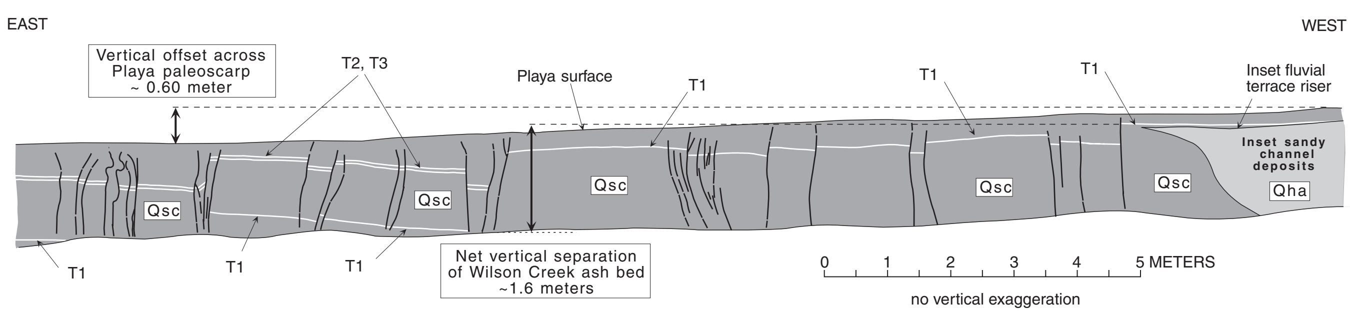

Figure 5. Sketch log (view to south) of channel exposure across Four Mile Flat fault zone ~100 m south of U.S. Highway 50. Map units: Qsc—Sehoo Alloformation; tephra-bearing clay deposits; Qha—inset Holocene sandy fluvial channel deposits. Qsc contains three tephra layers (white marker beds labeled T1-T3) each ~1–2 mm thick. based on glass chemistry analysis, the lowermost tephra layer (T1) correlates with the 14.7 ka Wilson Creek ash bed 4 (Sarna-Wojcicki, personal commun.). A tephra couplet (two layers separated by ~8 cm) (T2 and T3) stratigraphically overlies T1 by 0.8–1.0 m. The higher tephra of the couplet (T3) appears to correlate with one of any number of mid to late Holocene Mono Craters tephra (eastern California) (Sarna-Wojcicki, personal commun.). However, this correlation is problematic because the exposed section reveals no evidence for a stratigraphic discontinuity that would be expected within deposits spanning period(s) of lake desiccation in the Holocene. For simplicity, we regard the section as representing Sehoo age (latest Pleistocene) deposits. T1 is offset vertically approximately 1.6 m across the fault zone. The playa surface is offset vertically by only 0.6 m. These relations require a sequence of events as follows: 1) a faulting event that produced a ~1.0 m scarp and that postdates deposition of the 14.7 ka T1 tephra and younger strata; 2) erosional leveling of the playa surface; and 3) a second faulting event responsible for the 0.6 m scarp on the playa surface.

communication) and are reworked from pluvial Lake Lahontan and younger sediments. The quartz sands have been introduced to the Carson Sink by way of the Carson River and also by eolian processes evidenced by large active sand dunes that occupy the crest of the Blow Sand Mountains ~15 km to the south.

Drive by Stop #2b Fairview Site Historical Landmark

Directions: Continue east along U.S. Highway 50 for 13.7 mi (22 km).

This is the site of the old mining town of Fairview, which boomed ca. 1905–1907 as a result of rich silver discoveries. At its peak, the town had a population of 2000 with hotels, banks, 27 saloons, and a newspaper. The town and nearby mines were active until ca. 1917. Since then the area has been removed or destroyed. All that remains now is a concrete bank vault standing as a monolith on the horizon.

Stop 3. Overview of the Fairview Peak–Dixie Valley rupture sequence

Directions: Continue east along U.S. Highway 50 for 2.8 mi (4.5 km) to "Earthquake Faults" sign; turn south on dirt road; continue for ~100 m and park on the shoulder; you are on the 1954 Fairview Peak rupture trace.

The December 16, 1954 M_s7.2 Fairview Peak earthquake was followed 4 min and 20 sec later by the M_s6.8 Dixie Valley earthquake. Surface ruptures were distributed among six different faults that define a complex zone of normal and normal right-oblique surface ruptures 100 km long and >15 km wide (Fig. 3) (Slemmons, 1957; Caskey et al., 1996) The sequence progressed from south to north and initiated on the east-dipping Fairview fault. Surface ruptures on the Fairview fault extend for a distance of 32 km and exhibit primarily right-oblique displacements. A maximum right-lateral offset and vertical separation of 3.4 and 3.8 m, respectively, were measured near the epicentral region for the earthquake, just south of Fairview Peak (Fig. 3). The subsequent Dixie Valley earthquake produced a 46-km-long rupture along the east-dipping Dixie Valley fault, which bounds the eastern escarpment of the Stillwater Range. In contrast to the Fairview fault, the Dixie Valley fault ruptures produced only dip-slip offsets. Maximum vertical separations of ~2.8 m were measured along two distinct reaches of the fault, one just north of Coyote Canyon, near the south end of the main rupture trace, and near IXL Canyon (Fig. 3). Because the Dixie Valley event occurred only 4 min after the Fairview Peak earthquake, details of the Dixie Valley waveforms are obscured by those of the preceding event. Hence, efforts to locate the Dixie Valley epicenter have been problematic (Doser, 1986) (Fig. 3) and first motion data are not available to constrain a focal mechanism for the event.

The west-dipping West Gate, Louderback Mountains, and Gold King faults also ruptured during the sequence, although these fault ruptures are of relatively short length (10, 14, and 8.5 km, respectively). The West Gate and Louderback Mountains ruptures produced maximum right-oblique-slip offsets of 1.4 and 1.8 m, respectively. The Gold King fault ruptures showed only dip-slip offsets averaging ~0.5 m. The Gold King fault also produced minor surface ruptures during the 1903 Wonder earthquake (Slemmons et al., 1959). Although, there were no eyewitness reports to confirm whether the west-dipping faults ruptured with the first or second earthquake, it is generally assumed that the Fairview fault and faults along the eastern side of Dixie Valley ruptured with the initial Fairview Peak event. This interpretation is corroborated somewhat by the balance of moment release calculated from geologic data for the two events (Caskey et al., 1996). The three west-dipping faults form a complex structural linkage within a 15 km left-step between the east-dipping Fairview and Dixie Valley faults (Figure 6). The west-dipping faults appear to have played an important role in the transfer of stress and subsequent triggering of the Dixie Valley earthquake (Caskey and Wesnousky, 1997) (discussed at Stop 7). Finally, in the northern part of Gabbs Valley, minor ruptures broke along a 6-km-long portion of the Phillips Wash fault (south of area shown in Fig. 3) during the 1954 sequence. Curiously, the Phillips Wash ruptures trend subparallel to the Fairview fault, yet they produced left-oblique displacements.

During the summers of 1992 and 1993, the entire rupture zone was traversed and mapped on sets of ~1:12,000 scale, low-sun-angle aerial photos taken in 1968 and 1970. A total of ~600 measurements of vertical separation and lateral offset were made at intervals averaging ~300 m along-strike for each fault trace. Many of the observations and analyses made during the course of the Caskey et al. study form the basis for discussions at some of the stops on this field trip.

Overview of Quaternary stratigraphy in the Fairview Peak–Dixie Valley–Stillwater seismic gap area

A series of late Quaternary chronostratigraphic units was differentiated by Bell and Katzer (1987) in the central Dixie Valley area, and they provide the stratigraphic framework for interpreting and comparing the paleoseismic histories of the several fault zones in the region extending between Fairview Peak on the south and the Stillwater seismic gap on the north. Eight principal stratigraphic units are defined, ranging in age from mid Pleistocene (100–200 ka) to modern (Fig. 7). A sequence of alluvial fan-piedmont deposits are distinguished based on soil-geomorphic characteristics, the presence of chemically distinct volcanic tephra, and stratigraphic position relative to latest Pleistocene lake deposits.

Old alluvial-fan deposits (Qfo) occur as dissected fan-piedmont remnants preserved along range fronts and locally on broad uplifted piedmont slopes. The deposits typically exhibit strongly developed argillic Bt horzions overlying stage IV (Bqkm) carbonate horizons. These well-developed durargids and paleargids generally correspond to the Cocoon soil of Morrison (1964), estimated by Morrison and Davis (1984) to be of

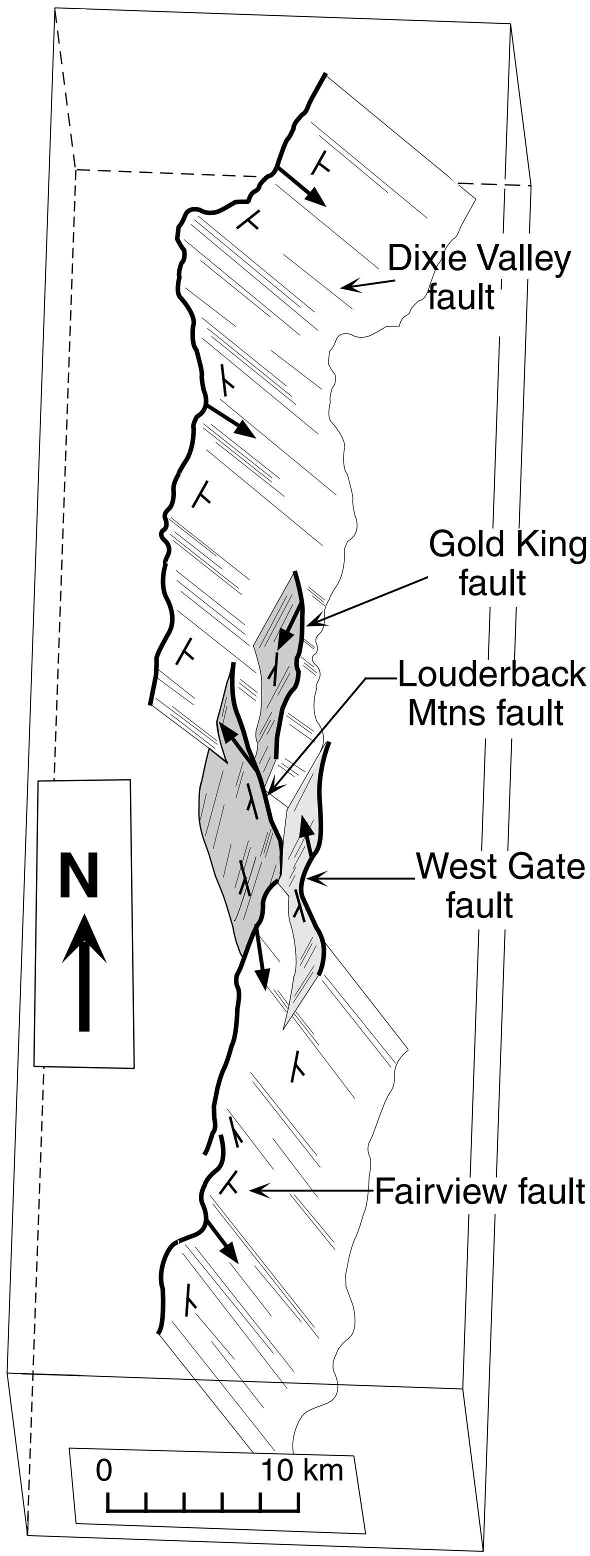

Figure 6. Schematic block diagram of the geometry of the December 1954 fault rupture system (with the exception of the Phillips Wash fault trace). Bold lines represent surface rupture traces. Bold arrows indicate the general direction of motion of hanging-wall blocks. Strike and dip symbols are shown for reference. West-dipping faults are gray (modified after Caskey et al., 1996).

oxygen-isotope stage 7 age (200 ka). The unit likely consists of multiple fan sequences covering a broad range of ages. No numerical age data have yet been obtained in this area, but the unit is estimated to range in age from stage 5 to 7 (100–200 ka).

Intermediate-age fan deposits (Qfi) are late Pleistocene in age based on their stratigraphic position below the pluvial Lake Dixie deposits. The fan deposits contain well-developed argillic Bt horizons and stage II-III Bk carbonate horizons, confirming that the unit predates the 12–13 ka highstand of Lake Lahontan according to the soil morphology studies of Nettleton et al. (1975).

At the main scarp of the Fairview Peak rupture (Stop 4), Qfi deposits contain the 35.4 ka Wilson Creek tephra bed 19 based on glass chemistry analysis by A. Sarna-Wojcicki (1998 data).

Lacustrine units Qbfo, Qbg, and Qbfy are associated with a Pleistocene pluvial lake that occupied central and northern Dixie Valley. Although the Dixie Valley–Fairview Peak area was not hydrologically connected to the Lake Lahontan drainage system, the area contained the contemporaneous pluvial Lake Dixie, providing a regional late Pleistocene stratigraphic datum. In central Dixie Valley, Thompson and Burke (1973) radiocarbon-dated two samples of calcareous tufa from high shoreline beach gravel deposits (Qbg) of Lake Dixie (elevation 1085–1090 m) and obtained ages of 11.6 and 11.7 ^{14}C ka. Similarly, recent new dates obtained by the authors place a maximum age of the highstand at 11.4 ka. The old basin fill deposits (Qbfo) mapped by Bell and Katzer (1987) were inferred to be older lacustrine deposits, and the young basin fill deposits (Qbfy) were determined to be partly contemporaneous and partly younger than Qbg. The upper Qbfy deposits contain Mazama ash (6.85 ka) and are likely associated with shallow lake and subaerial deposition.

The mottled alluvial fan deposits (Qfm) derive their name from the distinctive speckled or mottled appearance of the fan surfaces on aerial photography, produced by localized bioturbation of the well-developed desert pavement. The Qfm fan deposits occur extensively across the alluvial piedmonts, burying and beveling Qbg and older deposits. Although the oldest Qfm deposits appear correlative with the highest Qbg deposits, they are mostly younger than the shoreline gravels, and upper Qfm deposits overlie Mazama ash; the unit thus appears to contain several subunits ranging in age from mid-Holocene to latest Pleistocene (6.85–11.7 ka). Soils in Qfm deposits typically exhibit cambic Bw and stage I–II carbonate Bk horizons, although locally the B horizons are incipient to weak argillic (Btj) horizons owing to the strong influx of Na-rich dust from the valley floor.

The young alluvial fan deposits (Qfy) are as areally extensive as the Qfm deposits, covering large portions of the alluvial piedmonts. They consist of numerous, coalescing debris- and flood-flow deposits ranging in age from mid- to late Holocene. Soils in Qfy typically contain weak cambic Bw and Stage I carbonate Bk horizon. The Qfy deposits in Dixie Valley contain several late Holocene Mono Craters tephra beds, including the

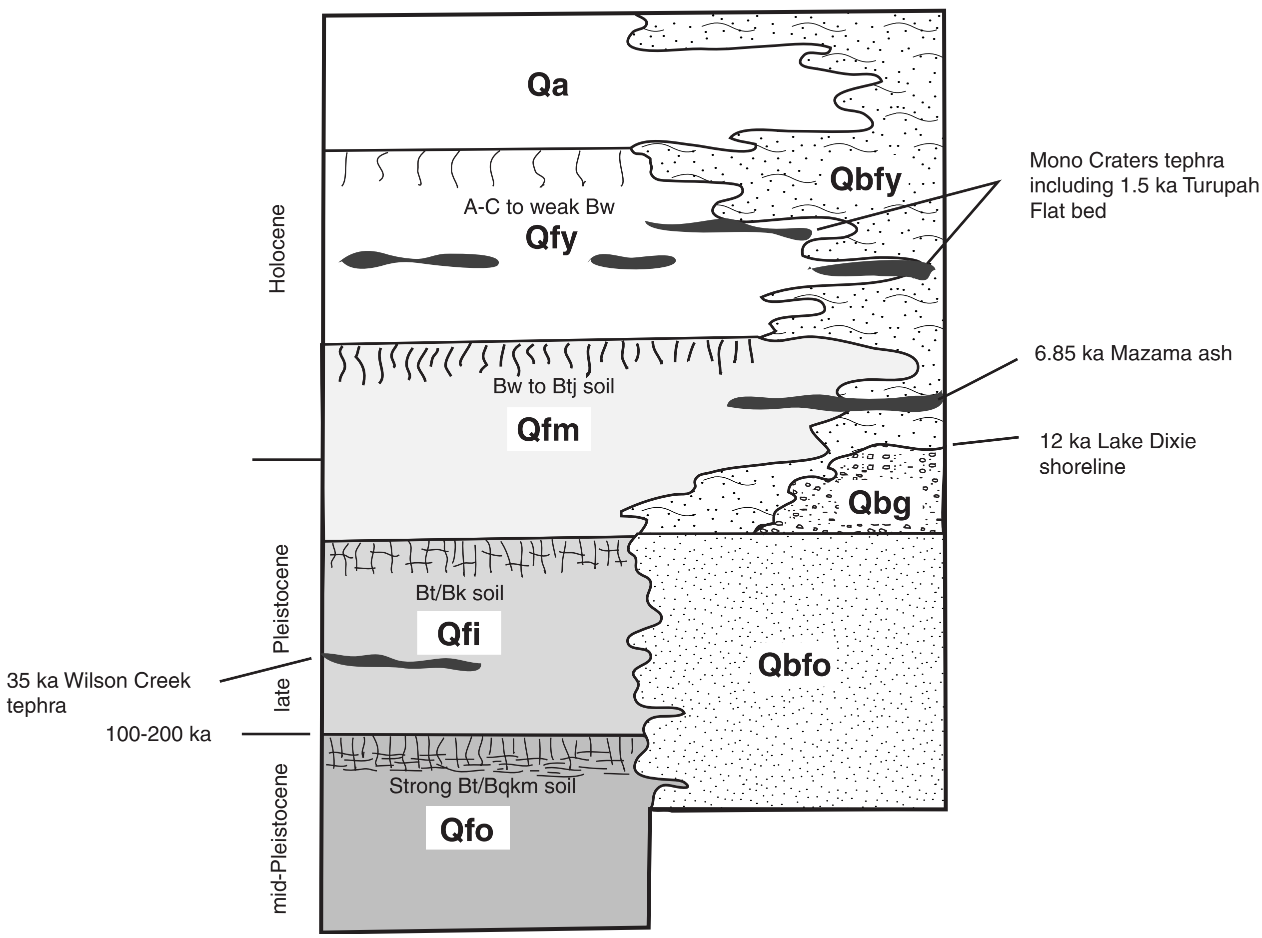

Figure 7. Generalized stratigraphic column showing chronostratigraphic units in the Fairview Peak and Dixie Valley region (after Bell and Katzer, 1987).

Turupah Flat tephra, a 1.5 ka volcanic ash that is ubiquitously found in most drainages in the Dixie Valley–Fairview Peak area.

Stop 4. Main scarp of the Fairview Peak rupture

Directions: Continue south from Stop 3 along Fairview Peak road for 5.0 mi (8.0 km); turn west up the large wash on a small dirt road that ends at the fault scarp in a turn-around parking area.

This portion of the 1954 Fairview Peak rupture, informally known as the “main site,” is on the northern segment of the Fairview fault; to the south of the main site, the fault rupture steps left into Bell Flat. The main site exhibits some of the largest displacements associated with the earthquake (Fig. 8a) and provides key paleoseismic data bearing on the long-term slip history of the fault. Based on measurements made shortly after the earthquake, Slemmons (1957) described offsets at the main site ranging up to 2.1 m vertical, 3.4 m right-lateral, and 4.1 m net slip (Fig. 9). Recent mapping by Caskey et al. (1996) documented numerous other sites exhibiting similar components of right-lateral offset. These offsets together with the development of graben in the steeply sloping offset fan surfaces account for the unusually large (7 m) and fresh-looking scarps still visible at the site.

The alluvial fan deposits offset by the fault at the main site are Qfy and Qfi (Fig. 3); to the north Qfm deposits comprise the faulted piedmont. The large scarp across the wash in the parking area is in Qfy deposits, and fan surfaces into which the drainages are deeply incised are all of Qfi age, containing strong argillic Bt and stage II–III Bk horizons. To the south, the scarp ascends a high Qfi remnant that exhibits still visible 2 m right-lateral offset of the narrow ridge crest. Slemmons (1957) measured offset roots and striations at this location having a rake of 55° south.

Detailed surficial mapping of the faulting in the main site revealed no evidence for older scarps in the Qfi alluvium. In 1998 an exploratory trench was excavated across the 4 m Fairview Peak scarp south of the main site, and the trench provided verification that Qfi deposits were offset only by the 1954 rupture. At the distal end of the offset fan, Qfi deposits exposed in the road cut contain a 3–5 cm tephra layer identified as the Wilson Creek bed 19, radiocarbon dated in the Mono Lake area at 35.4 ka (A. Sarna-Wojcicki, unpub. data). The presence of the ash together with the lack of evidence for prior faulting in the

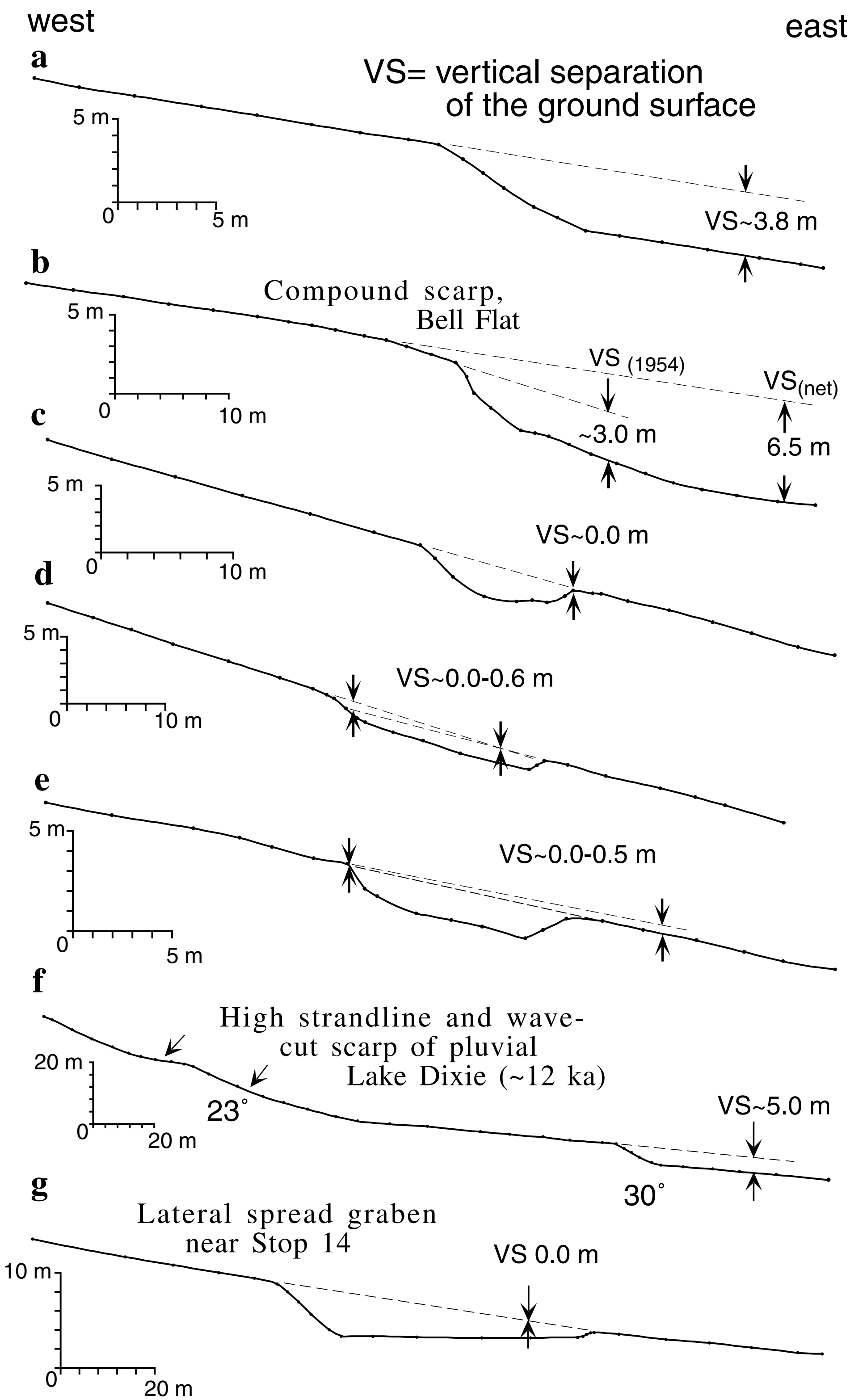

Figure 8. Scarp profiles referred to in text (Caskey et al., 1996; Caskey, unpublished data); a) maximum vertical separation along the Fairview fault, b) compound scarp north end of Bell Flat, d)–f) graben profiles between Little and Big Box canyons along the Dixie Valley fault, f) wave cut strandline and "Bend event" scarp (with scarp slope angles shown) for comparison) (Stop 13), and g) lateral spread graben near Stop 14.

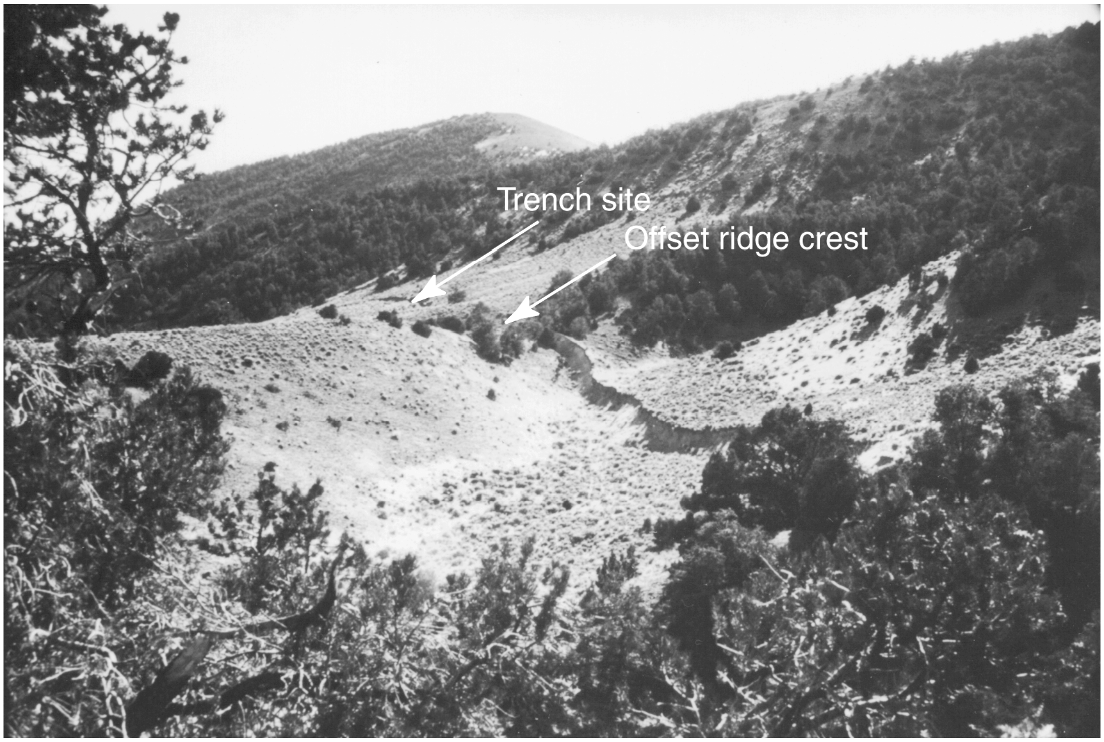

Figure 9. Photograph looking south along the Fairview Peak scarp at the main site showing the location of the right-lateral ridge crest offset and the site of the exploratory trench (photograph by D.B. Slemmons, 1966).

Qfi deposits indicate that the Fairview fault had not ruptured for at least 35 ky prior to 1954.

Stop 5. Compound scarp in northern Bell Flat

Directions: Continue south on Fairview Peak road from main site for 2.2 mi (3.6 km); the 1954 scarp is located ~100 m west of the road.

At this location in northern Bell Flat, the 1954 rupture lies along a 1 km left-step in the Fairview fault zone (Fig. 10). Qfi and younger deposits are offset only by the 1954 rupture, but remnants of the older Qfo fan deposits are offset by the 1954 and one additional older event forming a compound scarp with 6.5 m of net vertical separation (Fig. 8b). Vertical separation associated with the earlier event (~3.5 m) was comparable in size to that in 1954 (~3.0 m) (Fig. 8b). Qfm deposits are vertically separated across a single event 1954 rupture by ~2.3 m several hundred meters north of the profile shown in Fig. 8b. Caskey et al. (1996) identified as much as 2.5 m of right-lateral offset near this site, but comparable lateral offsets related to the older event are not evident.

The penultimate event therefore predates the 35.4 ka Qfi deposits and postdates Qfo deposits estimated to be between 100–200 ka in age. The age estimate for Qfo deposits thus provides an approximate maximum limiting age for the event. The lack of prehistoric faulting in Qfi deposits and the evidence for a single earlier event in Qfo deposits indicate that the Fairview fault is a low slip rate fault (<0.1 mm/yr).

DAY 2. DIXIE VALLEY: LA PLATA CANYON TO THE BEND

Stop 6. La Plata Canyon fault scarp

Directions: From Fallon, head east along U.S. Highway 50 from U.S. Highway 95 intersection for 40 mi (64 km) to State Highway 121 turn north. From Stop 5, return to U.S. Highway 50, head west for 1.8 mi (2.9 km) to State Highway 121 turn north. Proceed north for 2.7 mi (4.3 km) to intersection of dirt roads marked by a sign to Wonder, a mining camp located in the Louderback Mountains to the northeast; take the dirt road that heads northwest and continue 6.8 mi (10.9 km) across southern Dixie Valley to the La Plata Canyon fault scarp.

The La Plata Canyon fault is one of several parallel faults located in the left step-over region between the 1954 Fairview Peak and Dixie Valley rupture zones (Fig. 3). Although it did not rupture in 1954, it exhibits one of the largest Holocene scarps in the region, and it is considered an important structure for understanding the temporal and spatial pattern of faulting in this part of the CNSB. Map relations suggest that the La Plata Canyon fault may be structurally connected with the Sand Springs Range fault to the south.

The scarp at this location is ~2 km in length and ~7 m in height, cutting Qfm fan deposits (Fig. 11). Topographic profiles across the scarp indicate that the Qfm fan surface has 5 m of vertical separation. Unpublished surficial mapping by Luca Guerrieri in 1998 indicated that Qfm consists of two distinct

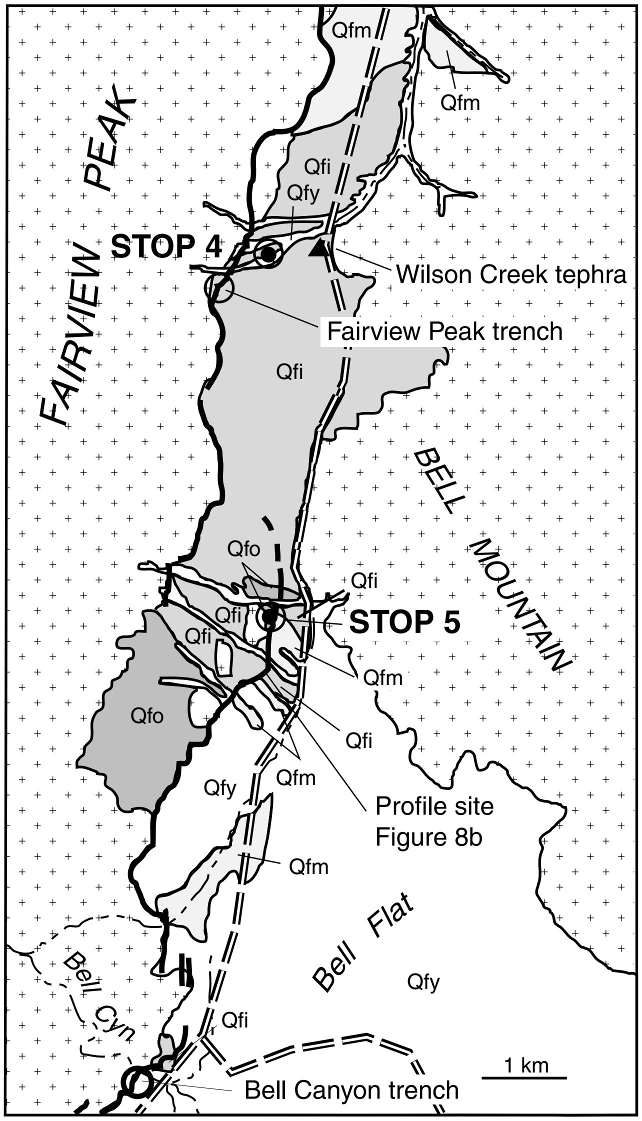

Figure 10. Generalized surficial geologic map showing the 1954 Fairview Peak rupture traces between the main site and Bell Flat.

fan surfaces at this location, the younger fan being inset 1–2 m below the older surface. Qfy fan deposits occur as wash terraces inset into Qfm, and they are offset by a 0.3–1.0 m high scarp.

An exploratory trench across the fault at this site (Fig. 12) revealed faulted Qfm alluvial fan deposits and a stacked sequence of four colluvial wedge deposits. The three oldest colluvial wedges account for most of the measured offset; they are separated from the most recent wedge by an incipient argillic (Btj) soil horizon. The youngest colluvial wedge is associated with the most recent 0.5–1.0 m scarp. Although numerical age dates have not yet been obtained from Qfm deposits exposed in the trench, the regional stratigraphic relations indicate that the four faulting events are younger than the high shoreline of Lake Dixie, ~11–12 ka, with the most recent event probably occurring in the last ~1 ka. These relations suggest that average slip rates are on the order of 0.4–0.5 mm/yr, which is considered a minimum collective rate for the several parallel faults in the La Plata Canyon area.

Stop 7. The Louderback Mountains fault ruptures, Holocene paleoscarp, and discussion o static stress changes and earthquake triggering during the December 16, 1954, sequence

Directions: Return to State Highway 121 (Dixie Valley Road) and turn north; continue 5.5 mi (8.8 km) to cattle gate along fence line to the east; proceed through gate on jeep trail; jeep trail crosses wash and turns north for ~1.0 mi, and eventually east up a dry wash; proceed up wash for another ~1.0 mi.

The Louderback Mountains fault (LMF) trace extends for a distance of 14 km along the west side of the Louderback Mountains (Fig. 3). Surface ruptures along the fault can be traced south to within ~100 m of the north end of the Fairview fault ruptures. This particular fault strand and several strands to the north were not mapped in Slemmon's original (1957) study. 1954 surface displacements on the LMF were dominantly right-lateral, and reach upwards to 1.0–1.5 m on this strand. The laterally offset geomorphic features along this section of the fault are not the best-preserved examples for the LMF, but the most accessible.

At this location, the LMF ruptures broke along a well-preserved paleoscarp that exhibits up to ~1.5 m of vertical separation. The paleoscarp is developed on dissected fan deposits that probably correlate with older variety Qfm deposits of Bell and Katzer (1987, 1990), based on the well-developed desert pavement, the mottled appearance of the fan surface on air photos, and relatively weak soil development. This implies that the paleoscarp is early Holocene or younger. Additionally, the deep erosional down-cutting of the fan unit and the similar deep dissection of older fan units and local pediment surfaces observed elsewhere in this region are a relatively recent geomorphic response to changes in climatic, and probably to some extent, tectonic conditions.

The detailed field observations of Caskey et al. (1996) describing fault geometry and both the amount and sense of slip along each fault of the rupture sequence provided the basis to examine three-dimensional static stress changes and earthquake triggering during the rupture sequence (Caskey and Wesnousky, 1997). Using the approach of Reasenberg and Simpson (1992) and Stein et al. (1992), static stress changes resulting from slip on individual fault ruptures were calculated for different stages of the northward propagating sequence. The primary results of the study can be summarized as follows: 1) Static stress changes imposed by rupture of the Fairview Peak earthquake are in the correct sense to explain the northward propagation of faulting along the four distinct faults that comprise the Fairview Peak earthquake and subsequent triggering of the Dixie Valley earthquake; 2) The Louderback Mountains and the Gold King faults

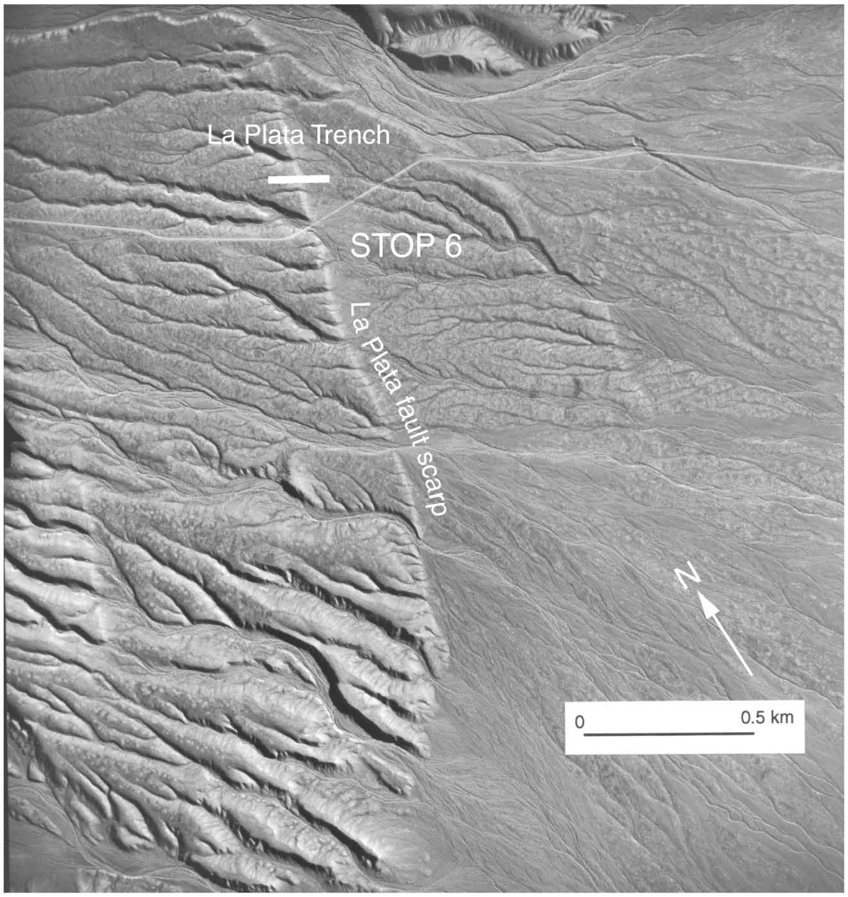

Figure 11. Low-sun-angle aerial photograph of the La Plata Canyon scarp showing the location of the exploratory trench.

played an important role in the transfer of stress change and triggering of the Dixie Valley earthquake; 3) The location of rupture endpoints correspond to areas where stress changes acted to inhibit rupture propagation. Hence, the stress changes may have played a role in controlling the extent of fault ruptures; and 4) The largest coseismic surface displacements tend to correlate with those sections of the faults showing the largest positive stress change (generally >4–6 bars) from preceding ruptures. The observations raise the interesting possibility that slip was not merely triggered, but that localized large stress changes may have somehow prepared the fault in such a way as to allow for greater coseismic slip locally during rupture.

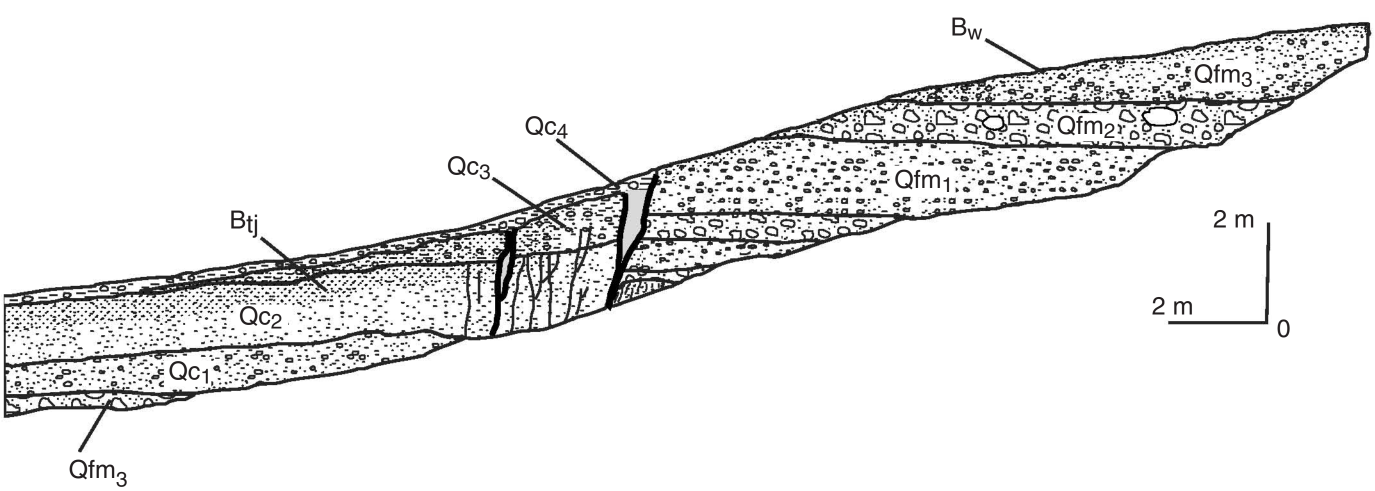

Figure 12. Exploratory trench log at La Plata Canyon (see Fig. 11 for location).

Stop 8. Big Box–Little Box Canyon scarps: Geologic and geophysical evidence for low dip on the Dixie Valley fault

Directions: Return to Dixie Valley Road and continue north 14.6 mi (23.5 km); turn west on jeep trail; proceed along jeep trail to Stillwater Range front at Big Box Canyon.

Despite a growing body of geological and geophysical evidence arguing for the existence of active low-angle normal faults in seismogenic crust (e.g., McDonald, 1976; Johnson and Loy, 1992), the paradox of the near-complete absence of low-angle normal faulting events in the seismic record remains. Caskey et al. (1996) reported data and a number of observations that strongly suggest that at least a 15–20-km-long section of the Dixie Valley fault rupture (between just north of Coyote Canyon and The Bend (Fig. 3) broke along a low-angle fault (~25–30°). Many of those observations are well-expressed along the range front ruptures between Little Box and Big Box canyons (Fig. 13) including: 1) a prominent low-angle fracture set within Tertiary granitic footwall rocks; The low-angle fractures parallel the entire sinuous range front trace from north of Coyote Canyon to just south James Canyon (Fig. 3) where the footwall rocks change to metasedimentary rocks; 2) graben profiles showing greater heave (fault normal extension) than vertical separation (Fig. 8c–e); This relation requires that the fault dips <45°. Balanced cross-sectional models of a graben at East Job Canyon, 3 km to the northwest, suggest that fault dip shallows in the subsurface to a dip of 25°–30°. 3) Three-point solutions for fault line elevation surveys at Little Box Canyon and James Canyon (Fig. 14).

Abbott et al. (in review) conducted seismic reflection and gravity experiments in the piedmont area of Willow Canyon (Fig. 3) to test the low-angle fault hypothesis of Caskey et al. (1996). The results of both high and medium resolution reflection surveys show profiles of a smooth fault plane dipping at 25°–30° to depths of 50 m and 500 m, respectively (e.g., Fig. 15). The medium resolution profile also shows stratigraphic truncations, hanging wall rollovers, and a slightly listric fault geometry (shallowing to <25°) at 1–2 km depths. Gravity profiles constrain a conservative maximum basin depth and define an essentially identical low-angle subsurface fault geometry to depths of >2 km. Unless the Dixie Valley fault becomes steeper at greater depths (which seems unlikely since it appears to show listric geometry above 3 km depth), then the results appear to mark the first on-land example of a historical large magnitude earthquake rupturing on a low-angle normal fault.

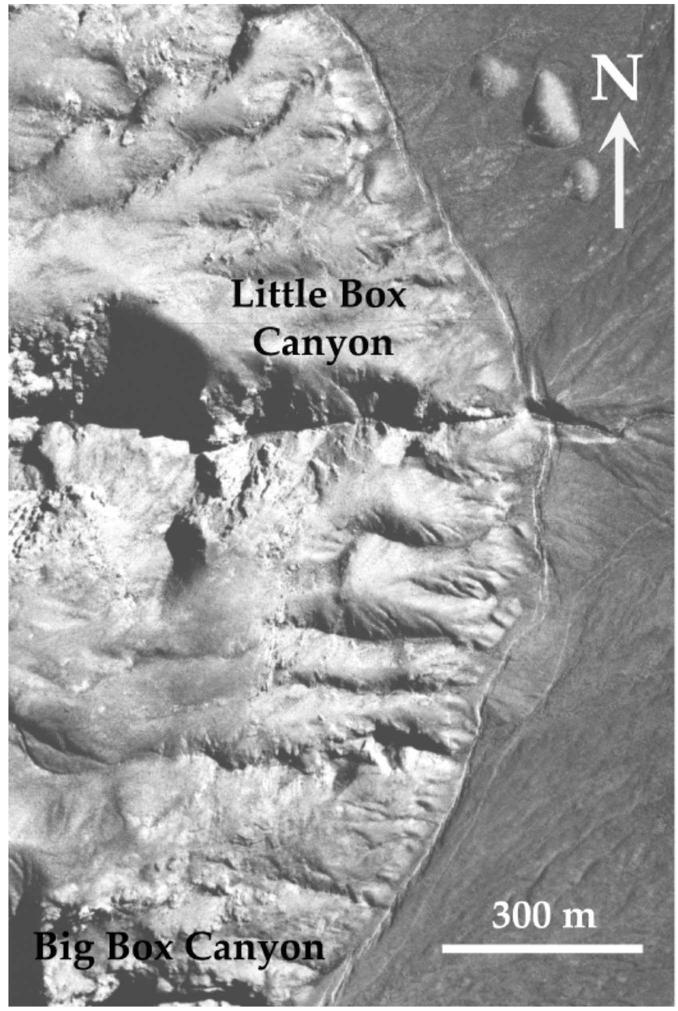

Figure 13. Low-sun-angle photograph of the Dixie Valley Range front surface ruptures in the vicinity of Little Box and Big Box Canyons. Note the well-developed fault trace grabens and left- and right-stepping en echelon scarp patterns north and south of The Bend in fault trace at Little Box Canyon. Scale is approximately 1:12,000.

Stop 9. Mazama Ash Exposure

Directions: Return to Dixie Valley Road and continue north 1.3 mi (2.1 km); turn east on Cattle Road; proceed for 0.4 mi (0.6 km).

The channel incision at this location exposes thick deposits of Mazama tephra (6.85 ka). The Mazama ash provides an important marker in the region for sorting out absolute and relative ages of surficial deposits as well as the timing of Holocene paleoseismic activity. The ash is also useful for deciphering important information regarding paleoclimatic fluctuations in the Holocene. For example, at this location, and also along Dixie Settlement Road, ~4 km to the north, Mazama ash lies within fluvial deposits. At the northern site, the tephra lies at an elevation of 1055 m (3460 ft). Approximately 15 km farther north, at Dixie Hot Springs the Mazama ash lies within what appear to be lacustrine deposits at an elevation of 1046 m (3430 ft) (Stop 12). These relations indicate that a sizable lake, with a high stand that reached an elevation between 3430 and 3460 ft (1046–1055 m), occupied Dixie Valley at 6.85 ka. This translates to a water depths of 15–24 m. We can therefore infer that the Great Basin was probably experiencing a slightly cooler and/or wetter climate during the time of the Mt. Mazama eruption.

Stop 10. IXL Canyon Fault Scarp

Directions: Continue north along Dixie Valley Road 2.7 mi (4.3 km); turn west; take south (left) fork in road and proceed

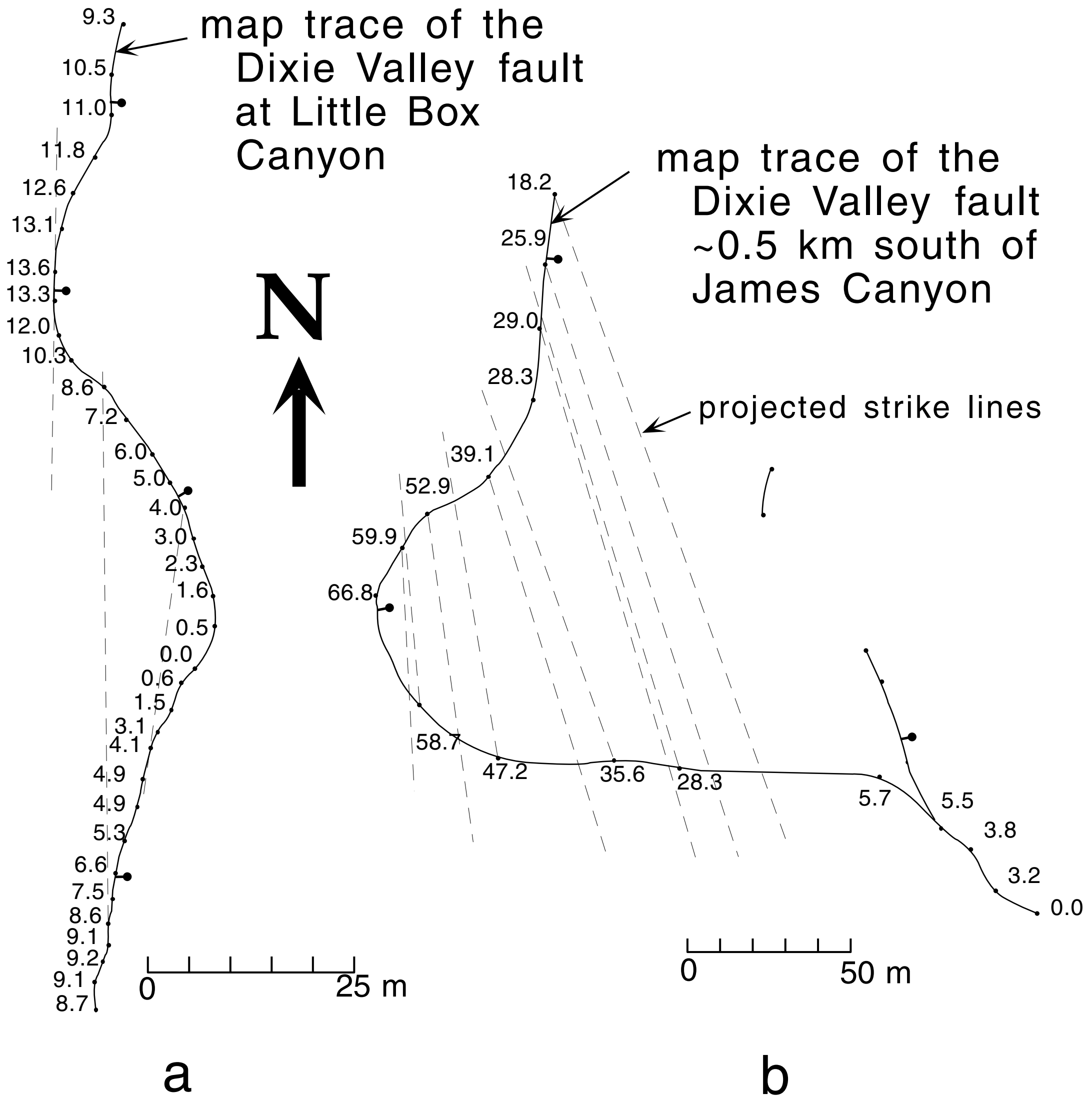

Figure 14. Fault line surveys along the Dixie Valley fault at (a) Little Box Canyon and (b) about 0.5 km southeast of James Canyon (Fig. 3). Survey points are show with their respective relative elevations in meters. The fault line at Little Box Canyon (a) lies entirely within alluvium. Three point solutions suggest that fault dip is ~32° at Little Box Canyon between relative elevations of 8.6 m and 0.5 m, and 20°–30° near James Canyon within the 65 m of elevation of the survey area.

2.1 mi (3.3 km) to range front fault scarp at the mouth of IXL Canyon.

The Stillwater Range is uplifted along a normal fault, here called the range-front fault, and along a series of synthetic, antithetic, and nested graben faults lying a few kilometers to the east, collectively called the piedmont fault zone (Fig. 16; Bell and Katzer, 1987). From the turnoff at Settlement Road, the dirt road to IXL Canyon crosses the piedmont fault zone ~0.9 km east of the range front where prominent scarps and graben as much as 15 m in height cut Qfo alluvial fan surfaces (Fig. 17). The 1954 event produced 3.5–4.0 m high scarps on the range front fault (1.5–2.5 m of vertical separation; Caskey et al., 1996) and 0–50 cm of offset on the piedmont scarps.

Paleoseismic studies in The Bend area (Bell and Katzer, 1990) indicated that late Quaternary faulting has migrated several times between the range-front and piedmont fault zones. The most recent event prior to 1954, termed The Bend event, occurred on the piedmont fault zone, and it produced 3 m high scarps comparable to those formed in 1954. In contrast to the 1954 rupture, however, surficial evidence indicated that no displacement occurred on the range-front fault during The Bend event. Other older events are preserved along the range-front fault, such as at IXL Canyon where Qfo deposits are offset ~12 m by pre-1954 faulting. North of IXL Canyon, Qfi fan deposits are offset by a single event that produced a 2.5–3.0 m high scarp; this event, which preceded The Bend event, is called the

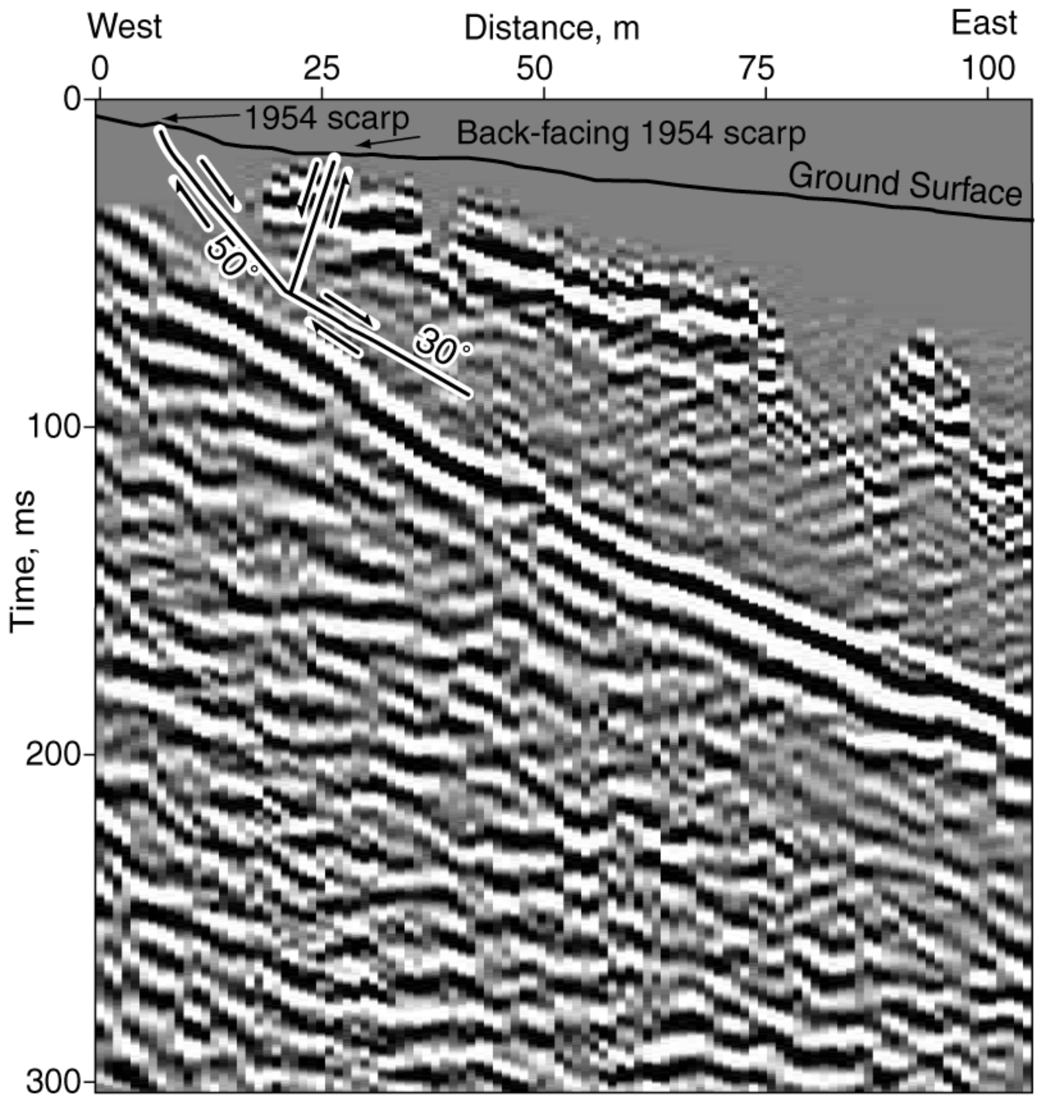

Figure 15. Common depth point (CDP) stack of high-resolution seismic reflection profile near the range front trace of the Dixie Valley fault near Willow Canyon (Abbott et al., in review) (Fig. 3). The Dixie Valley fault is represented by the prominent reflector that dips ~30° between 40–150 ms, and shallows to <25° below 150 ms. Note that there is no vertical exaggeration to the profile. The superimposed line drawing is from a balanced cross sectional profile of a graben at East Job Canyon (Caskey et al., 1996) ~2 km to the north.

IXL event and is the oldest mappable rupture in central Dixie Valley, extending the length of the 1954 rupture zone. Collective offsets on the range-front and piedmont faults associated with all events that cut Qfo and younger fan deposits indicate that late Quaternary slip rates are between 0.2–0.5 mm/yr.

DAY 3. THE BEND TO THE STILLWATER GAP

Stop 11. The Bend event fault scarp and 1954 liquefaction-related features

Directions: Return to intersection of Dixie Valley Road and Settlement Road (i.e., the turnoff to Stop 10); road turns to gravel; continue 3.2 mi (5.2 km) north along Dixie Valley Road; park on shoulder; hike ~400m west to small piedmont escarpment.

Some of the best examples of lateral spreads produced during the 1954 earthquake are expressed along the traverse from the road to piedmont fault scarp. Lateral spreads are liquefaction-induced structures that develop from down-slope movement of cohesive material atop a liquefied layer of large areal extent. The areas along the basin margin were highly susceptible to liquefaction during the 1954 event, evidenced by the formation of numerous sand boils and lateral spread features such as fissures, sinkholes, and small grabens. 1954 liquefaction-induced features formed discontinuously along the general fan piedmont-basin floor boundary for a distance of ~24 km (Slemmons, 1957;

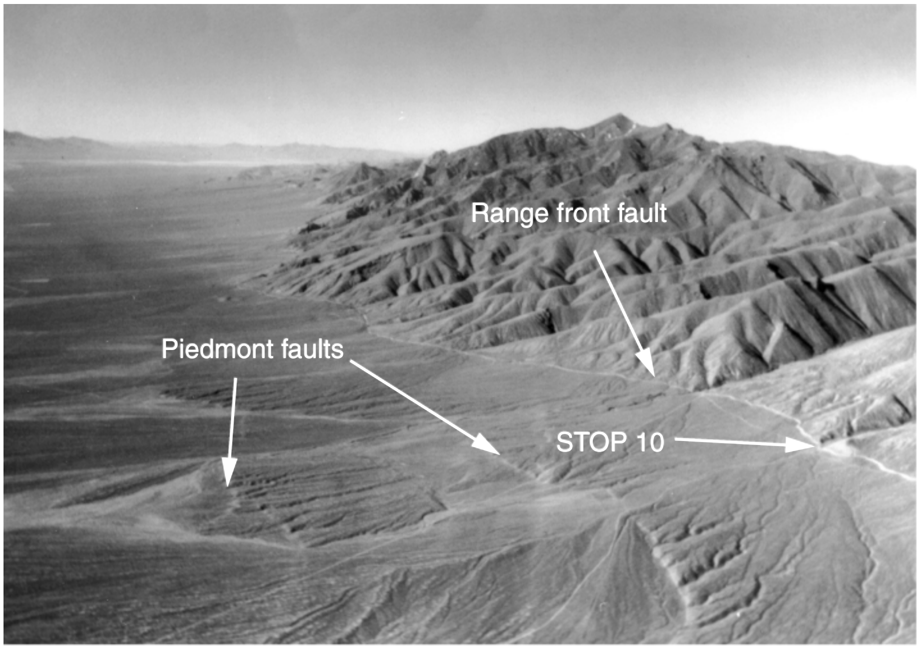

Figure 16. Oblique aerial photo of The Bend area along the Dixie Valley fault in the vicinity of Stop 10. View is to the southwest.

Caskey et al., 1996). Impressive as some of these 1954 features are, they are dwarfed in comparison to lateral spreads formed during the mid- to late Holocene Bend event. We'll observe examples of these Holocene features at Stops 12 and 14.

The 2–3 m scarp ~400 m west of the road is principally related to faulting produced by The Bend event, with =50 cm of that offset produced by 1954 faulting. The Bend event was associated with surface faulting that extended along the piedmont fault zone from Willow Canyon north into the Stillwater seismic gap, with an end-to-end length of at least 45 km and overlapping the 1954 rupture zone by ~22 km. Exploratory trenching on the scarp at this location and at the southern end of the rupture near Willow Canyon revealed that Qfm, Qbg, and lower Qfy deposits are offset 1.5–2.5 m by a single pre-1954 event. As discussed at the next stop, The Bend event produced much larger displacements in the Stillwater gap area where it is the only surface rupturing earthquake to have occurred in the last 12 ka. Surficial mapping by Bell and Katzer (1987) demonstrated that the age of The Bend event is bracketed by the Mazama and Turupah Flat ash beds (i.e., between 6.85–1.5 ka) from faulted Qfm and unfaulted Qfy deposits. The Bend event scarps typically exhibit steep scarp slope angles. Larger scarps to the north commonly lie at angle of repose for unconsolidated gravel (e.g., ~30°, Figure 8f). Diffusion equation models of The Bend event scarps suggest they may be as young as a few thousand years (Hecker, 1985; Pearthree, 1990).

Summary of paleoseismic data for the Dixie Valley–Fairview Peak fault zones

Results of event timing derived from paleoseismic studies in the 1954 Fairview Peak and Dixie Valley rupture areas show a widely diverse range in slip histories, and that the historical pattern of faulting does not mimic prehistoric patterns of faulting during ~the last ~100 ka. In central Dixie Valley, the penultimate event is dated at between 1.5–6.85 ka, and an older event is bracketed by the Qfm (<12 ka) and Qfi (35.4 ka) fan deposits; slip rates are on the order of 0.2–0.5 mm/yr. In contrast, the age of the penultimate event on the Fairview fault is at least 35.4 ka in age and apart from the 1954 rupture it is the only event to rupture the fault during at least the last ~100 ka. The late Quaternary slip rate of the Fairview fault is <0.1 mm/yr. The La Plata fault which[KB1] lies at the stepover between the Dixie Valley and Fairview Peak rupture zones did not rupture in 1954, but exhibits evidence for 4 faulting events in the last ~12 ka, the most recent probably occurring in the last ~1 ka. The minimum latest Pleistocene and Holocene slip rate for the La Plata fault is estimated at 0.4–0.5 mm/yr.

Although the historical pattern of faulting does not mimic recognizable prehistoric patterns, the available data cannot rule out previous Holocene temporal belt-like behavior. For example, multiple Holocene ruptures have occurred on the southern Dixie Valley fault (e.g., the La Plata site) and Four Mile Flat fault, and Holocene ruptures have occurred on the Louderback Mountains fault, the Stillwater gap segment of the Dixie Valley fault, and along the west side of the Stillwater Range (Dohrenwend et al. 1996; Caskey et al. 1996). Within our current level of resolution, we cannot rule out that these fault zones ruptured in a narrow time span during the past 1.5–6.85 ka (i.e., age of The Bend event).

The widely differing slip histories of historically active faults of the CNSB suggest that conventional paleoseismic parameters, such as slip rate and recurrence interval, may not be reliable criteria for distinguishing the hazards in the CNSB from other seismically active areas of the western Basin and Range. As noted by Bell et al. (1999), historically inactive faults lying outside of the CNSB have substantially higher slip rates. The

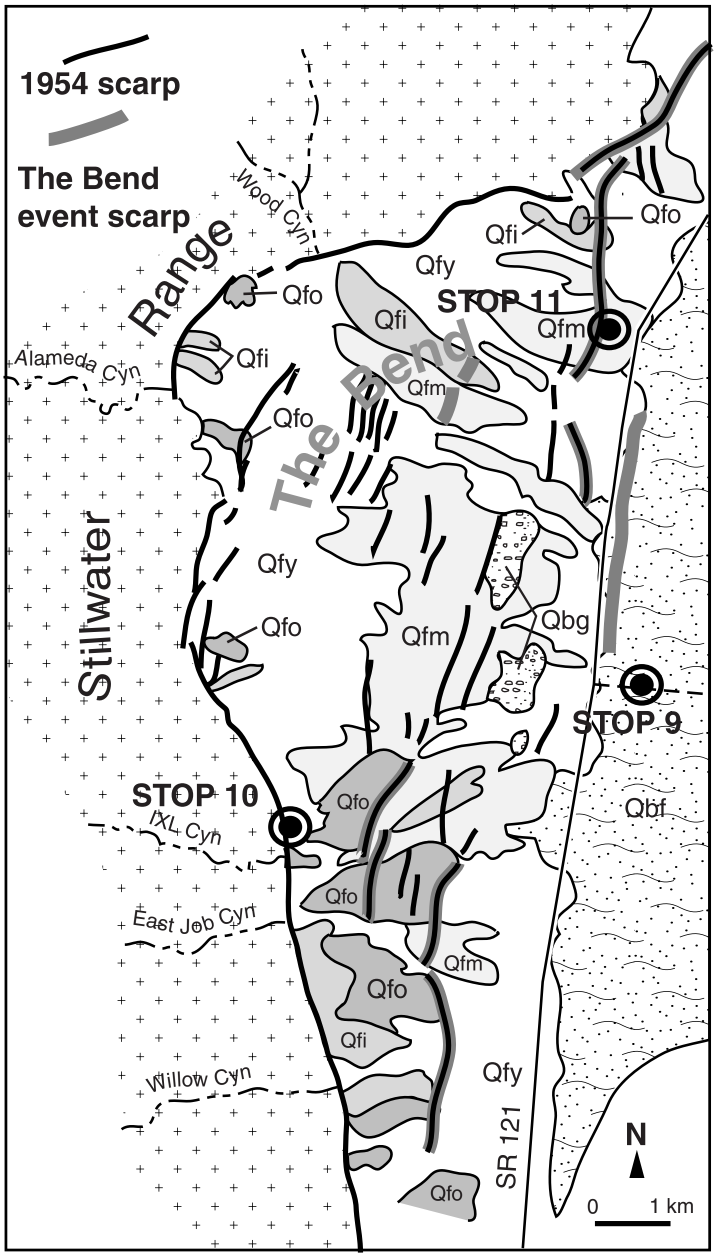

Figure 17. Dixie Valley surficial map.

<1 to <0.1 mm/yr slip rates estimated for faults in this portion of the CNSB are characteristic of many low- to moderate-slip rate normal faults in the western Basin and Range, and these rates are exceeded by those along other faults in the region, such as the Genoa fault which[KB2] exhibits a late Quaternary slip rate of 1–2 mm/yr (Ramelli et al., 1999).

Stop 12. Lateral Spread (?) Paleoscarps, Mazama Ash Exposure, Qfm Fan Deposits, and Northern Extent of the 1954 Rupture Zone

Directions: Continue 6.4 mi (10.3 km) north on Dixie Valley Road; park on road shoulder at dirt cross road from the east.

The large scarp at this location (Figure 18) is interpreted to be a lateral spread formed in response to liquefaction during the mid- to late Holocene Bend event rupture (1.5–6.85 ka). The isolated mound several meters west of the road exposes the stratigraphic section that is broken along the scarp. The section consists of Mazama ash-bearing lacustrine deposits overlain by Qfm fan deposits. The correlation of timing to The Bend event scarps is based on similar degrees of scarp preservation, proximity to The Bend event ruptures, and the fact that both are constrained to have occurred since the deposition of Mazama ash. The lateral spread interpretation is based on the scalloped-shaped nature of the scarps, an abundance of fissure-like scarp features within the footwall block, the distribution of

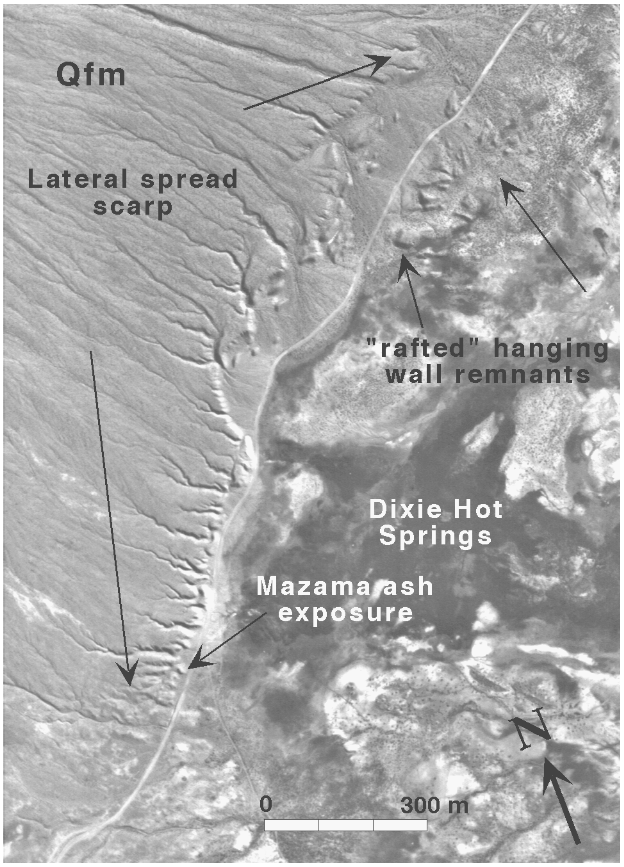

Figure 18. Low-sun-angle photograph of large lateral spread scarps near Dixie Hot Springs (Stop 12). Scale is ~1:12,000. See text for discussion.

fragmented blocks that emanate from the head scarps in apparent raft-like fashion (Fig. 18), the close proximity to the basin margin and high water table, and soft-sediment (liquefaction) features expressed locally on cleaned exposures of the disrupted sediments. Lateral spread paleoscarps of similar size formed along most areas along the fan piedmont-playa floor boundary, a distance of >20 km. In other cases the lateral spreads are mostly expressed as grabens, across which[KB3] there is no discernable vertical separation of the broken fan surfaces. What happened to the bulk of the hanging wall block at this location is problematic. However, the fragmented nature of hanging wall remnants and the irregular nature of landforms within the salt marsh to the east suggest that significant flow failure and subsidence may have accompanied liquefaction. Shoreline processes from subsequent, low-level lake stands may have also contributed to removing or obscuring hanging wall remnants.

The area along the range front at this location, marks the northernmost surface ruptures of the 1954 earthquake. Bend event paleoscarps are well preserved locally along the range front, and exhibit up to ~2 m of vertical separation along this section of the fault. Vertical separations across Bend event scarps increase to a maximum of ~5 m approximately 6 km to the north.

Stop 13. Stillwater Gap and surveys of pluvial Lake Dixie shorelines

Directions: Continue north on Dixie Valley Road 4.4 mi (7.1 km); park on road shoulder.

This location lies well within the Stillwater (seismic) gap (Wallace and Whitney, 1984), a 45 km-long section of the Dixie Valley fault (a.k.a. the Old Stillwater fault) that lies between the 1915 (M7.7) Pleasant Valley and 1954 (M6.8) Dixie Valley fault rupture zones to the north and south, respectively (Fig.1). Although the Stillwater Gap has not ruptured historically, Holocene scarps have been mapped discontinuously along most of its length. For example The Bend event ruptures overlap with the 1954 ruptures by ~22 km and have been mapped northward into the gap for at least another 23 km (Caskey and Wesnousky, 2000). The total length of 45 km together with an average slip for the event of ~2.0–4.0 m (Caskey, unpub. data) equate to an estimated moment magnitude of 7.1–7.3 for The Bend event. Holocene ruptures have also been mapped along the northernmost section of the fault (Wallace and Whitney, 1984; Fonseca, 1988; Pearthree, 1990; Caskey and Wesnousky, 2000). It is uncertain whether the scarps in northernmost Dixie Valley formed during The Bend event. However, scarp profile analyses of Pearthree (1990) suggest that the northernmost scarps may be slightly older than The Bend event scarps.

At this location Thompson and Burke (1973) surveyed elevations of high-level pluvial Lake Dixie shorelines at three sites along the range front to estimate net Holocene offsets and fault slip rates across the fault (Fig. 19). The southernmost shoreline lies within the footwall of the Dixie Valley fault and is marked by a cemented beach gravel strand line ~10 m above the base of the range front. The middle site consists of cemented beach gravel deposits that form a prominent beach terrace. Thompson and Burke (1973) interpreted this site to lie between two active strands of the fault. A piedmont strand broke during The Bend event rupture. This strand is clearly visible on the valley side of the terrace where it exhibits 5.0 m of vertical separation of the ground surface (Fig. 8f). The range front strand lies west of the bedrock knob on which the terrace is formed, and does not appear to show Holocene offset at that location (Caskey, unpub. data). Hence the beach gravel terrace, like the cemented beach gravel strand line to the south appears to lie entirely within the footwall of The Bend event ruptures. The northernmost shoreline is marked by rounded beach gravel deposits along the highest of a series of strand lines notched into older alluvial fan deposits.

Thompson and Burke (1973) concluded from their survey that the three shorelines (from south to north) lie at elevations of 1090 m (3574 ft), 1087 m (3566 ft), and 1080 m (3544 ft), suggesting a total vertical separation >9 m (30 ft). They interpreted this to mean that the shorelines were offset by two or

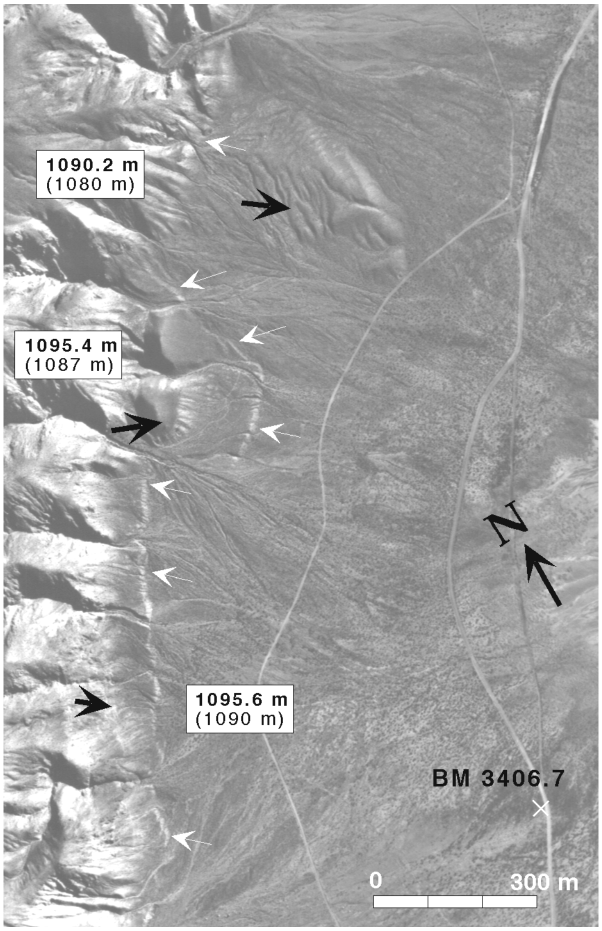

Figure 19. Low-sun-angle-photograph showing survey site and elevations of pluvial Lake Dixie shorelines (black arrows) of Thompson and Burke (1973) (values in parentheses) and Caskey et al. (in review) (values not in parentheses). Mid- to Late Holocene "Bend event" fault trace is marked by white arrows. Elevations of Caskey et al. were determined using a Total Station and calibrated to BM elev. 3406.7 (adjusted National Geodetic Survey elevation). See text (Stop 13) for discussion.

more episodes of post-Lake Dixie (post-12 ka) faulting. From this data, they calculated Holocene extension rates of ~1 mm/yr.

Thompson and Burke's (1973) results have been problematic because the tectonic geomorphology of scarps along the range front indicates the occurrence of only one post-Lake Dixie surface faulting event (i.e., The Bend event). Furthermore, maximum vertical offsets measured along Bend event ruptures are only 5–6 m (Caskey, unpub. data). For these reasons we resurveyed the three sites (twice) during summer 1999 using a Total Station. Contrary to the previous survey, our results showed that the three sites (from south to north) lie at elevations of 1095.6 m (3593.5 ft), 1095.4 m (3593.1 ft), and 1090.2 m (3575.9 ft), a net difference in elevation of only 5.4 m. Our recent survey results are therefore consistent with the post-Lake Dixie stratigraphic and structural relations along the fault and preclude the earlier, erroneously high extension rate calculations. The new data indicate a maximum extension rate of ~0.6 mm/yr (using similar geometric constraints as Thompson and Burke (1973)) averaged over an incomplete seismic cycle. This maximum rate is more in accord with rates averaged over similar and longer time intervals for the Dixie Valley fault (this study; Thompson and Burke, 1973; Bell and Katzer, 1990). Within the uncertainties associated with identifying "high-stand" shorelines, local tectonic effects, and possible influences from isostatic rebound of pluvial Lake Lahontan basin to the west (Adams and Wesnousky, 1999), Lake Dixie appears to have reached a high stand elevation of 1090–1095 m (3575–3590 ft).

Stop 14. Lateral spread graben and imbricated lake sediments

Directions: Continue north on Dixie Valley Road 1.8 mi (2.9 km); pull into graded area around conspicuous pipe (geothermal well); park; proceed on foot ~0.3 km southeast to edge of playa.

Approximately 1 km west of this location (Fig. 20) is a large lateral spread graben (Fig. 8g) that is interpreted to have formed during the mid to late Holocene Bend event. The graben is ~50 m wide. Valley-facing scarps along the graben are up to 8 m high. There is no discernible net vertical separation across the graben (Fig. 8g). Lateral spreads of this magnitude would seem to require the presence of downslope free faces, such as those found along stream banks or fault scarps, in order to allow for basin-ward movements. In this case however, downslope movement has apparently been accommodated by intense thrust

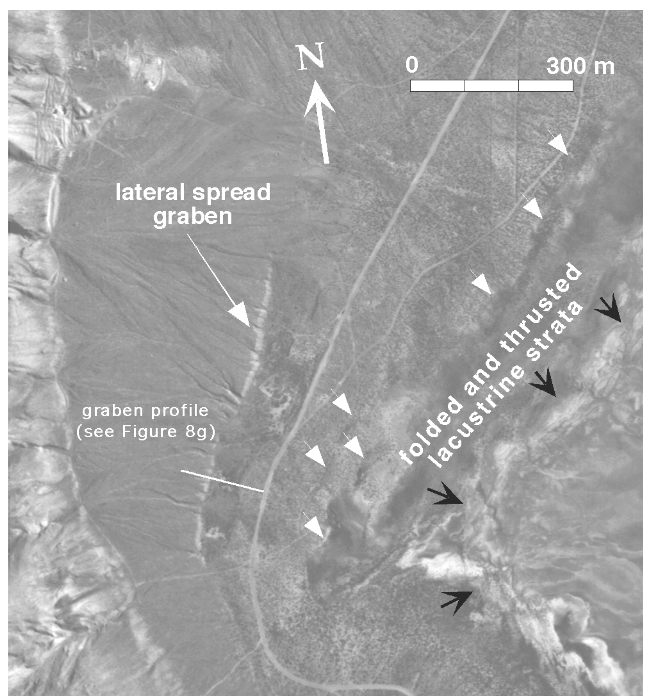

Figure 20. Low-sun-angle photograph of lateral spread graben and folded and thrusted lacustrine strata that fringes the playa margin. Other lateral spread features are marked by white arrows. Note the prominent "Bend event" scarps along the range front to the west. See text (Stop 14) for discussion.

imbrication and folding of lacustrine sediments along the playa margin (e.g., Obermeier, 1987). The elongate landforms that fringe the playa margin at this location (Fig. 20) are actually thin thrust sheets of lake deposits that contain the Mazama ash. The post-Mazama age constraint makes it likely that disruption of the lake sediments occurred contemporaneously with the lateral spreads and faulting along the range front. Mazama ash-bearing sediments are repeated at least 14 times across the disrupted zone, mostly above west-vergent thrust "faults." East of the zone of disrupted sediments, the Mazama ash lies at a shallow depth of 0.5 m below the surface, indicating that the detachment zone for the small "thrust belt" also lies at a very a shallow depth. The ash bed is almost everywhere associated with an overlying, well-indurated salt layer that has apparently given rigidly to the lake sediments and allowed for the somewhat regular "fold and thrust belt" geometry to develop. We find similarly deformed lake sediments everywhere along the playa margin where large-scale lateral spreads formed upslope. The large distances between lateral spread head scarps and disrupted lake sediments (up to 1.5 km) indicate the presence of a subsurface liquefied zone of enormous areal extent.

David B. Slemmons, Honorary Field Trip Leader

This field trip is dedicated to David B. "Burt" Slemmons, Professor Emeritus of Geology at the University of Nevada, Reno, for his pioneering work in active faulting and paleoseismology. Burt's active faulting studies began at many of the sites that will be visited on this field trip, and he will be contributing his historical observations to this trip as Honorary Field Trip Leader.

As a fresh Ph.D. graduate from the University of California, Berkeley, Burt began his career at the University of Nevada, Reno, in 1951 when he was hired as an Assistant Professor to teach courses as a "hardrock" instructor in petrology and petrography. At that time, Burt was also selected to supervise the University of Nevada Seismographic Station (now the Seismological Laboratory) of which he was the head from 1952–1964. When the series of ground-rupturing earthquakes occurred in the Rainbow Mountain, and Dixie Valley–Fairview Peak areas in 1954, Burt was one of the first geologists in the field mapping and documenting the surface faulting, as seen in this vintage photograph taken by Karl Steinbrugge in 1954 of Burt standing by the Fairview Peak scarp. His paper "Geological Effects of the Dixie Valley–Fairview Peak, Nevada, Earthquakes of December, 16, 1954" published in the Seismological Society of America Bulletin is a classic reference for anyone studying the contemporary tectonics of the Basin and Range Province. His research on the 1954 rupture zone contributed to his receiving the G.K. Gilbert Award in Seismic Geology from the Carnegie Institute in 1962.

During his subsequent years at Nevada, Burt continued to specialize in active fault research, perfecting his trademark methodology, the use of low-sun-angle aerial photography. He educated and advised dozens of undergraduate and graduate students (as well as colleagues), many of whom have gone on to become well-known neotectonics experts in teaching, research, and geotechnical consulting. Since retiring from the University of Nevada in 1989, Burt has continued to be active in various seismology research projects, including the assessment of seismic hazard at the proposed high-level nuclear waste repository site at Yucca Mountain. Burt and his wife Ruth presently live in Las Vegas, where Burt is studying the seismic activity of southern Nevada.

REFERENCES CITED

Abbott, R.E., Louie, J.N., Caskey, S.J., and Pullammanappalli, S., (in review), Geophysical confirmation of low-angle normal slip on the historically active Dixie Valley fault, Nevada: Journal of Geophysical Research.

Adams, K.A., and Wesnousky, S.G., 1998, Shoreline processes and the age of the Lake Lahontan highstand in the Jessup embayment, Nevada: Geological Society of America Bulletin, v. 110, no. 10, p. 1318–1332.

Adams, K.A., Wesnousky, S.G., and Bills, B.G., 1999, Isostatic rebound, active faulting, and potential geomorphic effects in the Lake Lahontan basin, Nevada and California: Geological Society of America Bulletin, v. 111, p. 1739–1756.

Anderson, L.W., and Hawkins, F.F., 1984, Recurrent Holocene strike-slip faulting, Pyramid Lake fault zone, western Nevada: Geology, v. 12, p. 681–684.

Bell, J., and Katzer, T., 1990, Timing of late Quaternary faulting in the 1954 Dixie Valley earthquake area, central Nevada: Geology, v. 18, p. 622–625.

Bell, J.W., 1984, Quaternary fault map of Nevada, Reno Sheet: Nevada Bureau of Mines and Geology Map 79.

Bell, J.W., and Bonham, H.F., 1987, Geologic map of the Vista 7.5′ quadrangle: Nevada Bureau of Mines and Geology Map 4Hg.

Bell, J.W., and Katzer, T., 1987, Surficial geology, hydrology, and late Quaternary tectonics of the IXL Canyon area, Nevada, as related to the 1954 Dixie Valley earthquake: Nevada Bureau of Mines and Geology Bulletin 102, 52 p.

Benson, L., Currey, D., Lao, Y., and Hostetler, S., 1992, Lake-size variations in the Lahontan and Bonneville basins between 13,000 and 9000 ^{14}C yrs. B.P: Palaeogeography, Palaeoclimatology, Palaeoecology, v. 95, no. 1–2, p. 19–32.

Caskey, S.J., and Wesnousky, S.G., 2000, Active faulting and stress redistributions in the Dixie Valley, Beowawe, and Brady's geothermal fields: Implications for geothermal exploration in the Basin and Range, *in* Proceedings, Twenty-fifth Workshop on Geothermal Reservoir Engineering, Stanford Geothermal Program Workshop Report SGP-TR-165, Stanford University, 16 p.

Caskey, S.J., Wesnousky, S.G., and Bell, J.W., (in review), Historic surface faulting and paleoseismicity in the vicinity of the 1954 Rainbow Mountain and Stillwater earthquake sequence, central Nevada: Bulletin of the Seismological Society of America.

Caskey, S.J., Wesnousky, S.G., Zhang, P., and Slemmons, D.B., 1996, Surface faulting of the 1954 Fairview Peak (Ms7.2) and Dixie Valley (Ms6.9) earthquakes, central Nevada: Bulletin of the Seismological Society of America, v. 86, no. 3, p. 761–787.

Caskey, S.J., and Wesnousky, S.J., 1997, Static stress changes and earthquake triggering during the 1954 Fairview Peak and Dixie Valley earthquakes, central Nevada: Bulletin of the Seismological Society of America, v. 87, no. 3, p. 521–527.

Davis, J.O., 1978, Quaternary tephrochronology of the Lake Lahontan area, Nevada and California, Nevada Archeological Survey Research Paper No. 7, 137 p.

Dohrenwend, J.C., Schell, B.A., Menges, C.M., Moring, B.C., and McKittrick, M.A., 1996, Reconnaissance photogeologic map of young (Quaternary and Late Tertiary) faults in Nevada, Open File Report, OFR 96–2: Nevada Bureau of Mines and Geology, in cooperation with the U.S. Geological Survey, scale 1:1,000,000.

Doser, D., 1986, Earthquake processes in the Rainbow Mountain–Fairview Peak–Dixie Valley, Nevada region 1954–1959: Journal of Geophysical Research, v. 91, p. 12572–12586.

Hecker, S., 1985, Timing of Holocene faulting in part of a seismic belt, west-central Nevada [M.S. thesis]: University of Arizona, 45 p.

Hodgkinson, K.M., Stein, R.S., and Marshall, G., 1996, Geometry of the 1954 Fairview Peak–Dixie Valley earthquake sequence from a joint inversion of leveling and triangulation data: Journal of Geophysical Research, v. 101, no. B11, p. 25,437–25,457.

Johnson, R.A., and Loy, K.L., 1992, Seismic reflection evidence for seismogenic low-angle faulting in southeastern Arizona: Geology, v. 20, no. 7, p. 597–600.

McDonald, R.E., 1976, Tertiary tectonics and sedimentary rocks along the transition: Basin and Range province to plateau and thrust belt province, Utah, *in* Symposium on geology of the Cordilleran hingeline, Denver, p. 281–317.

Morrison, R.B., 1964, Lake Lahontan: Geology of the southern Carson Desert, Nevada: U.S. Geological Survey Professional Paper 401, 156 p.

Morrison, R.B., 1991, Quaternary stratigraphic, hydrologic, and climatic history of the Great Basin, with emphasis on Lakes Lahontan, Bonneville, and Tecopa, *in* Morrison, R.B., ed., Quaternary nonglacial geology: Conterminous U.S.: Boulder, Colorado, Geological Society of America, The Geology of North America, v. K-2, p. 283–320.

Morrison, R.B., and Davis, J.O., 1984, Quaternary stratigraphy and archeology of the Lake Lahontan area: A reassessment, *in* Lintz, J., ed., Western geological excursions: Boulder, Colorado, Geological Society of America Annual Meeting Guidebook: Reno, Nevada, Mackay School of Mines, p. 252–281.

Naylor, M.A., Mandl, G., and Sijpesteijn, C.H.K., 1986, Fault geometries in basement-induced wrench faulting under different initial stress states: Journal of Structural Geology, v. 8, p. 737–752.

Pearthree, P., Fonesca, J., and Hecker, S., 1986, Patterns of Holocene and Quaternary faulting in the central Nevada seismic belt: Implications for fault behavior in the northern Great Basin: Geological Society of America Abstracts with Programs, v. 18, no. 2, p. 170.

Pearthree, P.A., 1990, Geomorphic analyses of young faulting and fault behavior in central Nevada [Ph.D. thesis]: University of Arizona, 212 p.

Pearthree, P.A., and Wallace, T.C., 1988, Evidence for temporal clustering of large earthquakes in central Nevada: Seismological Research Letters, v. 59, no. 1, p. 17.

Ramelli, A.R., Bell, J.W., dePolo, C.M., and Yount, J.C., 1999, Large-magnitude, Late Holocene earthquakes on the Genoa fault, west-central Nevada and eastern California: Seismological Society of America Bulletin, v. 89, no. 6, p. 1458–1472.

Reasenberg, P.A., and Simpson, R.W., 1992, Response of regional seismicity to the static stress change produced by the Loma Prieta earthquake: Science, v. 255, p. 1687–1690.

Sanders, C.O., and Slemmons, D.B., 1979, Recent crustal movements in the central Sierra Nevada–Walker Lane region of California–Nevada: Tectonophysics, v. 52, p. 585–597.

Slemmons, D.B., 1957, Geological effects of the Dixie Valley–Fairview Peak, Nevada, earthquakes of December 16, 1954: Bulletin of the Seismological Society of America, v. 47, no. 4, p. 353–375.

Slemmons, D.B., Steinbrugge, K.V., Tocher, D., Oakeshott, G.B., and Gianella, V.P., 1959, Wonder, Nevada, earthquakes of 1903: Bulletin of the Seismological Society of America, v. 49, no. 3, p. 251–265.

Stein, R.S., King, G.C.P., and Jian, L., 1992, Change in failure stress on the southern San Andreas fault system caused by the 1992 M7.4 Landers earthquake: Science, v. 258, p. 1328–1332.

Stewart, J.H., 1988, Tectonics of the Walker Lane belt, western Great Basin: Mesozoic and Cenozoic deformation in a zone of shear, *in* Ernst, W.G., ed., Metamorphism and crustal evolution of the western United States: Englewood Cliffs, New Jersey, Prentice-Hall, p. 683–713.

Stewart, J.H., and Carlson, J.E., 1978, Geologic map of Nevada: U.S. Geology Survey in cooperation with Nevada Bureau of Mines and Geology, scale 1:500,000.

Thatcher, W., Foulger, G.R., Julian, B.R., Svarc, S.L., Quilty, E., and Bawden, G.W., 1999, Present day deformation across the Basin and Range province, western United States: Science, v. 283, p. 1714–1718.

Thompson, G.A., and Burke, D.B., 1973, Rate and direction spreading in Dixie Valley, Basin and Range province, Nevada: Geological Society of America Bulletin, v. 84, p. 627–632.

Tocher, D., 1956, Movement on the Rainbow Mountain fault: Bulletin of the Seismological Society of America, v. 46, p. 10–14.

Wallace, R.E., 1984, Patterns and timing of Late Quaternary faulting in the Great Basin province and relation to some regional tectonic features: Journal of Geophysical Research, v. 89, no. B7, p. 5763–5769.

Wallace, R.E., and Whitney, R.A., 1984, Late Quaternary history of the Stillwater seismic gap, Nevada: Bulletin of the Seismological Society America, v. 74, no. 1, p. 301–314.

Printed in the USA.